Diffusion in a deformable lattice: Theory and numerical results

W. G. Kleppmann and R. Zeyher

Max-Planck-Institut für Festkörperforschung, Heisenbergstrasse 1, 7 Stuttgart 80, Federal Republic of Germany

(Received 3 December 1979)

We develop a transport theory of one-dimensional diffusion of a single particle in a three-dimensional deformable lattice with a Debye spectrum. Our treatment is based on the Mori formalism; the memory kernel is evaluated in the mode-mode coupling approximation. This allows us to evaluate the absolute magnitude of the diffusion constant, the frequency-dependent conductivity, and the incoherent neutron scattering cross section of the diffusing particle. The main results are: (a) The diffusion constant obeys an Arrhenius law at very low temperatures. At higher temperature $(k_B T \gtrsim \Delta E/4, \Delta E$ is the activation energy) the apparent activation energy increases with temperature. This increase depends on the mass M^A of the diffusing particle leading to an apparent activation energy that increases slightly with decreasing M^A. The prefactor (attempt frequency) shows only a very small dependence on M^A for not too small masses. As a result, the diffusion coefficient is nearly independent of M^A. Only for small M^A we recover the isotopic effect as predicted, for instance, by the theory of Vineyard. (b) The frequency-dependent conductivity $\sigma(\omega)$ shows a two-peak structure and a temperature dependence which is similar to that obtained in the Fokker-Planck treatments. The frequency of the upper peak of $\sigma(\omega)$ exhibits a square-root dependence on M^A whereas $\sigma(\omega)$ depends very little on M^A at low frequencies. Detailed results for the dependence on the elastic constant of the crystal and the masses of the particles are given. (c) Analogous results and plots have been obtained for the incoherent cross section of the diffusing particle.

I. INTRODUCTION

The diffusion of particles in solids has been studied by many authors over the last fifty years. The most famous examples are the diffusion of defects in metals[1,2] (for instance, hydrogen atoms in transition metals) and ionic conductors.[3,4] Recently the interest in diffusion problems has increased in connection with the rapid transport of ions occurring in superionic conductors.

The classical diffusion of a particle in a solid is a very complex theoretical problem. One difficulty is associated with the periodic potential experienced by the diffusing particle which is due to the periodic arrangement of the atoms of the solid. In almost all cases the difference between the maximum and the minimum of the periodic potential (activation energy ΔE) is large compared with $k_B T$. This makes the diffusion process thermally activated. The diffusion constant becomes $\sim e^{-\Delta E/k_B T}$ and thus obeys an Arrhenius law. Clearly this prevents any perturbational treatment since this would lead to a power series in T or in T^{-1}. The second difficulty is that the prefactor of the exponential, called attempt frequency, is a nonequilibrium quantity. Only in very special cases is it justified to approximate it by equilibrium quantities such as the curvature of the periodic potential near the extrema.[5]

There are two major theoretical approaches to particle diffusion in solids: The first one has been proposed by Vineyard[6] and refined by many authors.[1] The basic idea of this transition-state theory is to map the nonequilibrium aspect of the problem onto equilibrium quantities. It is assumed that the diffusion consists of discontinuous jumps of the system between the minima of the free energy over saddle points. The jump rate can be calculated from the expansion coefficients of the partition function around the saddle point in terms of generalized coordinates: The zeroth order yields the activation energy; the second-order coefficients are related to frequencies and yield, after a configurational average, the attempt frequency. In particular, the jump rate becomes $\sim M^{A-1/2}$ with M^A being approximately the mass of the diffusing particle. The second approach treats the nonequilibrium aspect of the diffusion process more correctly. A simple way to do this has been used in Ref. 7: The diffusing particle and all the other particles are interacting via harmonic forces. The irreversibility is introduced in an *ad hoc* way by the postulation of a breaking point where the harmonic band is destroyed and the particle jumps over the potential barrier. It is shown that in this model the diffusion constant is proportional to the inverse square root of M^A as it is in the transition-state theory. Reference 8 avoids the assumption of a breaking point by considering explicitly the nonlinear interaction between the normal modes. In this case the diffusion constant becomes proportional to the inverse square of M^A in contrast to the above theories. Dealing with a heavy diffusing particle and using a similar approach, Ref. 9 comes to the conclusion that the diffusion constant should be independent of M^A.

In view of the above disagreement we thought it worthwhile to reconsider the problem and to use a different method for the calculation. We

approximate the excitations of the lattice by harmonic phonons with a Debye spectrum. Moreover we consider only a single mobile particle which is restricted to move in one dimension. Starting from a Hamiltonian we calculate the self-correlation functions of fluctuations in the density and momentum of the diffusing particle using the Mori method[10-12] and the mode-mode coupling approximation for the memory kernel. Clearly such an approach is superior to the first approach mentioned above: It keeps the general Hamiltonian but avoids the assumption of an equilibrium state in the saddle-point configuration. Actually the only approximation of the present approach is the mode-mode coupling assumption for the calculation of the memory kernel. In the absence of any small parameter it is hard to justify such an assumption *a priori*. However, it has been shown that this assumption gives excellent results in the case of anharmonic solids[13] and simple fluids.[14] By studying the neglected terms in the memory function we will demonstrate that at least for small temperatures $k_B T \ll \Delta E$ our assumptions yield reliable numerical results. In Sec. II we define our model Hamiltonian and derive the form of the imaginary part of the memory function in mode-mode coupling theory. This is compared with the Fokker-Planck result and related to experimental quantities. In Sec. III we present the details of the numerical calculations. The numerical results are shown and discussed in Sec. IV. The conclusions are summarized in Sec. V.

II. FORMALISM

A. Model

Our aim is to calculate the self-correlation function of a mobile particle in a deformable lattice. In the absence of interactions between the diffusing ions, it is sufficient to consider a single mobile ion. We assume that the Hamiltonian H of our system can be written as the sum of three terms

$$H = H^A + H^B + H', \tag{1}$$

where

$$H^A = \frac{p^2}{2M^A} + \sum_l V(x\vec{e}_x - \vec{x}^{(0)}(l)) \tag{2}$$

represents the part which depends only on the mobile particle A. p is its momentum, M^A its mass, and V represents the interaction potential of the mobile ion with a lattice ion in its equilibrium position $\vec{x}^{(0)}(l)$. The summation goes over all lattice ions l. In writing (2) we have assumed that the mobile ion is restricted to move in the x direction, i.e., only x coordinates of A are considered. Correspondingly, only xx correlation functions can be calculated.

$$H^B = \sum_l \frac{\vec{p}(l)^2}{2M^B} + \frac{1}{2} \sum_{l_1, l_2; \alpha_1, \alpha_2} \Phi^{(2)}_{\alpha_1 \alpha_2}(l_1, l_2) u_{\alpha_1}(l_1) u_{\alpha_2}(l_2) \tag{3}$$

is the part of the Hamiltonian that depends only on the lattice ions. We assumed that a harmonic description of this part is sufficient, since the lattice particles B (mass M^B) are bound to a time-independent equilibrium site. $u_\alpha(l)$ is the momentary displacement of the particle at site l in direction α from this site. The lattice particles can move in all three directions.

$$H' = \sum_{l, \alpha} V^{(1)}(x, l) u_\alpha(l) \tag{4}$$

represents the coupling between the mobile particle A at x and the displacements of the lattice particles. $V^{(1)}(x, l)$ is the first derivative of the lattice potential V of (2) with respect to x. In writing (4) it was assumed that it is sufficient to include only the terms to lowest order in the displacements of the lattice ions, whereas the part depending on the coordinates of A is retained fully. The advantage of this form of the coupling is that the effects of the lattice relaxation on the effective potential "felt" by the diffusing ion can be included exactly. This will be done explicitly later.

In nature there are several ionic conductors in which the mobile ions are restricted to one dimension, whereas the lattice vibrations are three-dimensional, e.g., β-eucryptite or hollandite,[3,4] to which our model applies directly. Furthermore one-dimensional diffusion models are often used as simplest theoretical systems to describe diffusion in solids.[15-18]

We now introduce real normal coordinates of the lattice ($\vec{q} > 0$ means that the summation is restricted to one-half of the Brillouin zone):

$$u_\alpha(l) = \left(\frac{2}{N}\right)^{1/2} \sum_{\vec{q}>0} \left[Q\binom{\vec{q}}{\alpha} \cos[\vec{q} \cdot \vec{x}(l)] + Q\binom{\vec{q}}{\alpha+3} \sin[\vec{q} \cdot \vec{x}(l)] \right], \tag{5}$$

or

$$Q\binom{\vec{q}}{\alpha} = \left(\frac{2}{N}\right)^{1/2} \sum_l u_\alpha(l) \cos[\vec{q} \cdot \vec{x}(l)], \quad Q\binom{\vec{q}}{\alpha+3} = \left(\frac{2}{N}\right)^{1/2} \sum_l u_\alpha(l) \sin[\vec{q} \cdot \vec{x}(l)]. \tag{6}$$

With $P(\vec{q}_\alpha) = M^B Q(\vec{q}_\alpha)$ one gets

$$H^B = \sum_{\vec{q}>0,\alpha}\left[P^2\binom{\vec{q}}{\alpha}\Big/2M^B + P^2\binom{\vec{q}}{\alpha+3}\Big/2M^B\right] + \frac{1}{2}\sum_{\vec{q}>0;\alpha,\beta}D_{\alpha\beta}(\vec{q})\left[Q\binom{\vec{q}}{\alpha}Q\binom{\vec{q}}{\beta} + Q\binom{\vec{q}}{\alpha+3}Q\binom{\vec{q}}{\beta+3}\right] , \qquad (7)$$

where

$$D_{\alpha\beta}(\vec{q}) = \sum_l \Phi_{\alpha\beta}(l)\cos[\vec{q}\cdot\vec{x}(l)] \qquad (8)$$

and

$$H' = \left(\frac{2}{N}\right)^{1/2}\left\{\sum_{\vec{q}>0,\alpha}\left[V^{(1)}\left(x,\binom{\vec{q}}{\alpha}\right)Q\binom{\vec{q}}{\alpha}\right.\right.$$
$$\left.\left. + V^{(1)}\left(x,\binom{\vec{q}}{\alpha+3}\right)Q\binom{\vec{q}}{\alpha+3}\right]\right\}, \qquad (9)$$

where

$$V^{(1)}\left(x,\binom{\vec{q}}{\alpha}\right) = \sum_l \frac{\partial V(x\vec{e}_x - \vec{x}(l))}{\partial x_\alpha(l)}\cos[\vec{q}\cdot\vec{x}(l)], \qquad (10)$$

$$V^{(1)}\left(x,\binom{\vec{q}}{\alpha+3}\right) = \sum_l \frac{\partial V(x\vec{e}_x - \vec{x}(l))}{\partial x_\alpha(l)}\sin[\vec{q}\cdot\vec{x}(l)].$$

Since in many cases it is more convenient to deal with complex coordinates, we also define these by

$$\tilde{Q}\binom{\vec{q}}{\alpha} = \left[Q\binom{\vec{q}}{\alpha} + iQ\binom{\vec{q}}{\alpha+3}\right]\Big/\sqrt{2},$$

$$\qquad (11)$$

$$\tilde{P}\binom{\vec{q}}{\alpha} = \left[P\binom{\vec{q}}{\alpha} + iP\binom{\vec{q}}{\alpha+3}\right]\Big/\sqrt{2} = iM^B\mathcal{L}\tilde{Q}\binom{\vec{q}}{\alpha},$$

where $\mathcal{L}$ is the Liouvillian ($\mathcal{L} = -i\partial/\partial t$) of the system. $\vec{q}$ now takes positive and negative values. With these the Hamiltonian becomes

$$H^B = \sum_{\vec{q},\alpha}\tilde{P}^2\binom{\vec{q}}{\alpha}\Big/2M^B + \frac{1}{2}\sum_{\vec{q},\alpha,\beta}D_{\alpha\beta}(\vec{q})\tilde{Q}^*\binom{\vec{q}}{\alpha}\tilde{Q}\binom{\vec{q}}{\beta} \qquad (12)$$

and

$$H' = \left(\frac{1}{N}\right)^{1/2}\sum_{\vec{q},\alpha}\vec{V}^{(1)}\left(x,\binom{\vec{q}}{\alpha}\right)\tilde{Q}\binom{\vec{q}}{\alpha}, \qquad (13)$$

where

$$\vec{V}^{(1)}\left(x,\binom{\vec{q}}{\alpha}\right) = \sum_l \frac{\partial V(x\vec{e}_x - \vec{x}(l))}{\partial x_\alpha(l)}\exp[-i\vec{q}\cdot\vec{x}(l)]. \qquad (14)$$

D remains real if every atom is at a center of inversion symmetry. Without restriction of generality we assume that D is diagonal in the indices α, β. Then one can, e.g., evaluate the partition function as ($j = \alpha$, $\alpha+3$)

$$Z = \int dx\, dp\, e^{-\beta H^A}\prod_{\vec{q},j}dQ\binom{\vec{q}}{j}dP\binom{\vec{q}}{j}e^{-\beta(H^B + H')}$$

$$= \left(\frac{2\pi}{\beta}\right)^{3N}(M^B)^{3N/2}\left(\prod_{\vec{q},j}D_{jj}^{-1/2}(\vec{q})\right)\left(\frac{2\pi M^A}{\beta}\right)^{1/2}$$

$$\times N\int_0^a dx\, e^{-\beta\bar{v}(x)}, \qquad (15)$$

where the effective potential is given by

$$\bar{v}(x) = \sum_l V(x\vec{e}_x - \vec{x}(l))$$

$$- N^{-1}\sum_{\vec{q},j}'\left[V^{(1)}\left(x,\binom{\vec{q}}{j}\right)\right]^2\Big/D_{jj}(\vec{q}). \qquad (16)$$

The correction term in (16) arises from a quadratic complement introduced to evaluate the integrals over $Q(\vec{q}_j)$ in (15).

From this partition function one can now evaluate various thermal expectation values, expressed as

$$\left\langle\!\!\left\langle\!\!\left\langle Q\binom{\vec{q}}{j}\right\rangle\!\!\right\rangle\!\!\right\rangle = Z^{-1}\int\prod_{\vec{q}',j}dQ\binom{\vec{q}}{j}dP\binom{\vec{q}}{j}dx\, dp$$

$$\times e^{-\beta H^A}Q\binom{\vec{q}}{j}e^{-\beta(H^B + H')}$$

$$= -\frac{1}{\beta}\left(\frac{N}{2}\right)^{1/2}Z^{-1}\partial Z\Big/\partial V^{(1)}\left(x,\binom{\vec{q}}{j}\right) = 0.$$

$$\qquad (17)$$

Since $V^{(1)}(x,(\vec{q}_j))$ is antisymmetric with respect to $x = 0$ and $\bar{v}(x)$ is symmetric,

$$\left\langle\!\!\left\langle\!\!\left\langle Q^2\binom{\vec{q}}{j}\right\rangle\!\!\right\rangle\!\!\right\rangle = -\frac{2}{\beta Z}\frac{\partial}{\partial D_{jj}(\vec{q})}Z = \int_0^a\left\{\frac{1}{\beta D_{jj}(\vec{q})} + \frac{2}{N}\left[V^{(1)}\left(x,\binom{\vec{q}}{j}\right)\right]^2\Big/D_{jj}(\vec{q})\right\}e^{-\beta\bar{v}(x)}dx\Big/\int_0^a dx\, e^{-\beta\bar{v}(x)}. \qquad (18)$$

B. Mori formulation

All correlation functions of interest can be expressed easily in terms of relaxation functions $\Phi_{ij}(z)$ for suitably chosen variables A_i and A_j (see subsection II. F).[12] The relaxation function is defined as

$$\Phi_{ij}(z) = \mp i \int_{-\infty}^{\infty} dt\, \Theta(\pm t)e^{izt}\langle A_i(t)|A_j(0)\rangle \quad \text{for Im}z \gtrless 0 ,$$

(19)

where

$$\langle A_i(t)|A_j(0)\rangle = \beta\langle\langle A_i*(t)A_j 0)\rangle\rangle$$

$$= \beta\langle\langle A_i(0)*e^{-i\mathcal{L}t}A_j(0)\rangle\rangle .$$

(20)

Substituting (20) into (19) we obtain

$$\Phi_{ij}(z) = \langle A_i|(z-\mathcal{L})^{-1}A_j\rangle ,$$

(21)

where we have written $A_i \equiv A_i(0)$. Mori showed that the relaxation function can be written as

$$\Phi_{ij}(z) = \sum_k [z - \Omega\chi^{-1} + M(z)\chi^{-1}]_{ik}^{-1}\chi_{kj} ,$$

(22)

where

$$\chi_{ij} = \langle A_i|A_j\rangle ,$$

(23)

$$\Omega_{ij} = \langle A_i|\mathcal{L}A_j\rangle ,$$

(24)

$$M_{ij}(z) = -\langle A_i\mathcal{L}Q|(z-Q\mathcal{L}Q)^{-1}Q\mathcal{L}A_j\rangle .$$

(25)

The operator Q is the projection operator onto the subspace of variables that has not been considered explicitly:

$$Q = 1 - P ,$$

(26)

$$P = \sum_{ij}|A_i\rangle\chi_{ij}^{-1}\langle A_j| .$$

(27)

The matrix χ is called the static susceptibility, Ω the frequency matrix, and M the memory matrix.

Equation (22) is an exact reformulation of Eq. (21) and nothing is gained as yet. There are two ways of proceeding from Eq. (22). Firstly, one can note that (25) has exactly the same form as (21), only the time evolution operator $\mathcal{L}$ is replaced by $Q\mathcal{L}Q$ (only the time evolution in the subspace not explicitly considered in the variables A_i contributes) and the variables are $Q\mathcal{L}A_i$ instead of A_i (only states orthogonal to the original states A_i contribute). By choosing a new subspace for $|Q\mathcal{L}A_i\rangle$ the procedure can be repeated, leading to a continued fraction expansion for Φ.

The alternative procedure, which we are going to follow, is to choose a set of variables A_i to be considered explicitly and assume that the influence of the other variables on the A_i can be described by a well-behaved and smooth $M(z)$ for which it is easier to make reasonable approximations, for instance, perturbation theory or a multimode expansion.[14] In Sec. II. E we are going to show that this approach is a generalization of the Fokker-Planck method in the sense that there one also chooses a set of relevant variables A_i and represents the rest of the system by a white-noise force and frequency- and position-independent damping, whereas we are going to calculate both frequency and spatial dependence of the damping and its magnitude within the so-called "mode-mode coupling approximation" (Sec. II. D). But before we can proceed we have to specify what variables we are going to consider explicitly as A_i. We are interested in the position-position and velocity-velocity self-correlation functions of the diffusing particle A; therefore we are going to choose its position and momentum:

$$n(k_x) = e^{ik_x X} ,$$

(28)

$$p(k_x) = e^{ik_x X} ,$$

(29)

where x is the momentary position of the diffusing particle and p its momentum. Higher powers of p will be ignored. In the following we will denote $n(k)$ by 1 and $p(k)$ by 2 in matrix notation. If, for the moment, one includes the lattice coordinates $Q(\vec{\alpha}{}^{\vec{q}})$ as 3 and $P(\vec{\alpha}{}^{\vec{q}})$ as 4, then from symmetry considerations one gets the following forms for χ and Ω:

$$\chi = \begin{bmatrix} \chi_{11} & 0 & \chi_{13} & 0 \\ 0 & \chi_{22} & 0 & 0 \\ \chi_{31} & 0 & \chi_{33} & 0 \\ 0 & 0 & 0 & \chi_{44} \end{bmatrix}$$

(30)

and

$$\Omega = \begin{bmatrix} 0 & \Omega_{12} & 0 & 0 \\ \Omega_{21} & 0 & 0 & 0 \\ 0 & 0 & 0 & \Omega_{34} \\ 0 & 0 & \Omega_{43} & 0 \end{bmatrix} .$$

(31)

Owing to the periodicity of the lattice and hence of the potential felt by the diffusing ion, one gets coupling between $n(k_x)$ and $p(k_x)$ with k vectors differing by multiples of the reciprocal-lattice vector in x direction. The coupling decreases rapidly with increasing reciprocal-lattice vector. Therefore, in the following only a small number is taken into account explicitly (5 to 15), the exact number N_0 being determined by the convergence of the calculation. χ_{11}, χ_{22}, Ω_{12}, and Ω_{21} are then

$N_0 \times N_0$ matrices in the reciprocal-lattice vectors. χ_{33}, χ_{44}, Ω_{34}, and Ω_{43} are 3×3 matrices in the Cartesian indices α, β, and χ_{13} is an $N_0 \times 3$ matrix.

If one defines

$$d(\vec{G}) = \langle e^{iG_x x} \rangle , \tag{32}$$

where $\vec{G}$ is a reciprocal-lattice vector, one can calculate χ and Ω easily as

$$\chi_{11}((k+G_1)_x, (k+G_2)_x) = \beta d(G_{1x} - G_{2x}) , \tag{33}$$

$$\chi_{22}((k+G_1)_x, \underline{(k+G_2)_x}) = M^A d(G_{1x} - G_{2x}) , \tag{34}$$

$$\chi_{33}\begin{pmatrix} \vec{k} \\ \alpha \quad \beta \end{pmatrix} = \delta_{\alpha\beta} D_{\alpha\alpha}^{-1}(\vec{k}) \int_0^a dx\, e^{-\beta \bar{v}(x)} \left\{ 1 + \beta N^{-1} \left[\vec{V}^{(1)}\left(x, \begin{pmatrix} \vec{k} \\ \alpha \end{pmatrix}\right) \right]^2 \middle/ D_{\alpha\alpha}(\vec{k}) \right\} \middle/ \int_0^a dx\, e^{-\beta \bar{v}(x)}$$

$$= D_{\alpha\alpha}^{-1}(\vec{k})\delta_{\alpha\beta} + O\left(\frac{1}{N}\right) , \tag{35}$$

$$\chi_{44}\begin{pmatrix} \vec{k} \\ \alpha \quad \beta \end{pmatrix} = M^B \delta_{\alpha\beta} , \tag{36}$$

$$\chi_{13}\left((k+G_1)_x, \begin{pmatrix} \vec{k} \\ \alpha \end{pmatrix}\right) = i\beta N^{-1/2} D_{\alpha\alpha}^{-1}(\vec{k}) \mathrm{Im} \left[\int_0^a dx \exp[-\beta\bar{v}(x) + i(k+G_1)_x x] \vec{V}^{(1)}\left(x, \begin{pmatrix} \vec{k} \\ \alpha \end{pmatrix}\right) \middle/ \int_0^a dx\, e^{-\beta\bar{v}(x)} \right] \tag{37}$$

$$\Omega_{12}((k+G_1)_x, (k+G_2)_x) = (k+G_1)_x d(G_{1x} - G_{2x}) = (k+G_2)_x d(G_{1x} - G_{2x}) + i\beta \sum_{G_x} K(G_x) d(G_{1x} - G_{2x} - G_x) \tag{38}$$

$$\Omega_{21}((k+G_1)_x, (k+G_2)_x) = (k+G_2)_x d(G_{1x} - G_{2x}) , \tag{39}$$

$$\Omega_{34}\begin{pmatrix} \vec{k} \\ \alpha \quad \beta \end{pmatrix} = i\delta_{\alpha\beta} , \tag{40}$$

$$\Omega_{43}\begin{pmatrix} \vec{k} \\ \alpha \quad \beta \end{pmatrix} = -i\delta_{\alpha\beta} , \tag{41}$$

where

$$K(x) = \sum_{G_x} K(G_x) e^{iG_x x} = -\frac{\partial \bar{v}(x)}{\partial x} . \tag{42}$$

C. Effective potential

We want to get as far as possible analytically, therefore we make some further simplifying approximations. Firstly, we assume that the harmonic lattice has a simple cubic structure with lattice parameter a and can be described adequately by a Debye spectrum

$$D_{\alpha\beta}(k) = M^B c^2 k^2 \delta_{\alpha\beta} . \tag{43}$$

Secondly, we assume that the interaction potential between a lattice ion and the mobile ion is described by a Gaussian

$$V(r) = A \exp(-Br^2) . \tag{44}$$

We do not expect that our results will depend sensitively on the detailed form of the potential (44) as long as the interatomic forces are short ranged.

One can then evaluate the effective potential for the diffusing ion explicitly by substitution into (16) to get

$$\bar{v}(x) = \sum_l A \exp\{-B[x\hat{e}_x - \vec{x}^{(0)}(l)]^2\}$$

$$- \frac{a^3}{4\pi^2 M^B c^2} \sum_{l_1, l_2} \frac{\mathrm{Si}[q_m | \vec{x}(l_1) - \vec{x}(l_2)|]}{|\vec{x}(l_1) - \vec{x}(l_2)|} 4A^2 B^2 \exp(-B\{[x\hat{e}_x - \vec{x}^{(0)}(l_1)]^2 + [x\hat{e}_x - \vec{x}^{(0)}(l_2)]^2\})$$

$$\times \sum_\alpha [x\hat{e}_x - \vec{x}^{(0)}(l_1)]_\alpha [x\hat{e}_x - \vec{x}^{(0)}(l_2)]_\alpha . \tag{45}$$
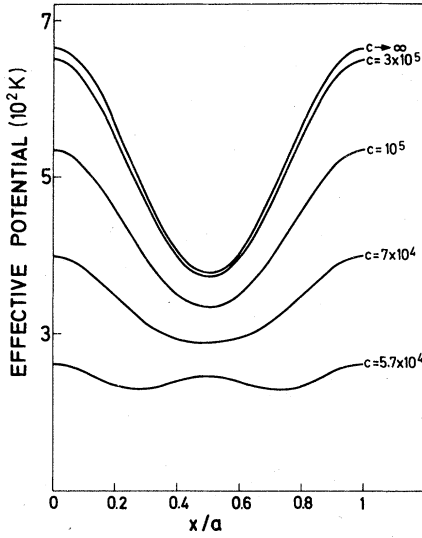
FIG. 1. Effective periodic potential seen by the diffusing ion for various sound velocities (cm/sec) with $A = 2000$ K, $B = 5/a^2$.

The first term in (45) arises from the direct interaction of A with all the lattice ions, the second term represents the effect of the lattice relaxation. It is always negative and hence leads to a reduction of the total energy, inversely proportional to $M_B c^2 =$ the elastic constant of the lattice. Furthermore it is $\sim A^2$, i.e., the square of the direct interaction strength, as is always the case in a linear coupling approximation. q_m is the maximum wave vector of the Debye spectrum and Si the sine integral function.

The activation energy for classical diffusion of A is given by $\bar{v}(0) - \bar{v}(a/2)$ (assuming that the lattice always relaxes to its equilibrium configuration for any position of A). The change due to the relaxation of the lattice is given by

$$\Delta E = - \frac{2a^4}{\pi^2 M^B c^2} A^2 B^2 \, e^{-Ba^2}(5.72 - 22.86 \, e^{-Ba^2/2}).$$

$$(46)$$

This shows that the activation energy increases if $Ba^2 < 2.77$, i.e., for a long-range interaction, and decreases otherwise. This behavior can be understood qualitatively by bearing in mind that the relaxation of the neighbors will be stronger for A at its saddle point than at its equilibrium position. If the interaction is short ranged, then the saddle-point energy gets reduced more than the equilibrium energy, $\Delta E > 0$. On the other hand, if the interaction is long ranged, then the energy reduction depends more on the number of relaxing neighbors than their displacements and $\Delta E < 0$. In Fig. 1 we compare the effective potentials for a particular choice of A, B, and a for different values of the elastic constants. In this case $Ba^2 = 5$ and this leads to a reduction of the activation energy with decreasing elastic constant. Mathematically this can be taken to the extreme of an almost vanishing activation energy (bottom curve), which in fact leads to a double-well potential. Reduction of the activation energy due to polarization effects, which are neglected here, have been discussed in Ref. 19.

One can now also give an explicit expression for χ_{13}. First we expand $\bar{V}^{(1)}(x, \binom{\vec{k}}{\alpha})$ in reciprocal-lattice vectors (bearing in mind the periodicity of $\bar{V}^{(1)}$) as

$$\bar{V}^{(1)}\left(x, \binom{\vec{k}}{\alpha}\right) = iAa^{-3}\left(\frac{\pi}{B}\right)^{3/2}$$

$$\times \sum_{\vec{G}} (k+G)_\alpha \, e^{-i(k+G)_x x} \, e^{-(\vec{k}+\vec{G})^2/4B}.$$

$$(47)$$

Substituting this expression into (37) we get

$$\chi_{13}\left((k+G_1)_x, \binom{\vec{k}}{\alpha}\right) = \frac{i\beta A}{\sqrt{N}\, M^B c^2 k^2 a^3}\left(\frac{\pi}{B}\right)^{3/2} \sum_{\vec{G}} (k+G)_\alpha \, e^{-(\vec{k}+\vec{G})^2/4B} \, d(\vec{G} - G_{1x}).$$

$$(48)$$

This form will be used in the explicit calculation of $M(z)$.

D. Mode-mode coupling approximation

Since we are interested only in the self-correlation functions for the diffusing ion, we restrict our attention to the subset of $n(k)$ and $p(k)$ of the variables considered in (30) and (31). The coupling to the lattice then only determines the memory functions (in a Brownian-motion language the lattice is the origin of the random force on the diffusing particle and the damping; however, we want to consider its influence more explicitly). The susceptibility and frequency matrices in (30) and (31) then become

$$\chi = \begin{pmatrix} \chi_{11} & 0 \\ 0 & \chi_{22} \end{pmatrix}, \quad \Omega = \begin{pmatrix} 0 & \Omega_{12} \\ \Omega_{21} & 0 \end{pmatrix}.$$

$$(49)$$

The memory kernel has the form

$$M = \begin{pmatrix} 0 & 0 \\ 0 & M_{22} \end{pmatrix}.$$ (50)

This follows immediately from considering the vertex in (25)

$$|Q\mathcal{L}n(k_x)\rangle = (ik_x/M^A)|Qp\rangle = 0.$$ (51)

Therefore the only nonvanishing part of the memory kernel becomes

$$M_{22}(z, (k+G_1)_x, (k+G_2)_x) = -\langle p((k+G_1)_x)\mathcal{L}Q|(z - Q\mathcal{L}Q)^{-1}Q\mathcal{L}p((k+G_2)_x)\rangle.$$ (52)

Our aim now is to find an approximation that allows us to calculate M_{22} explicitly from the known coupling to the lattice. To achieve this we have to make a number of approximations which we are going to summarize and discuss in the following:

(1) Only decay into product states of the original variables $n((k+G)_x)$, $p((k+G)_x)$, $\tilde{Q}(\begin{smallmatrix}\vec{\xi}\\\alpha\end{smallmatrix})$, and $\tilde{P}(\begin{smallmatrix}\vec{\xi}\\\alpha\end{smallmatrix})$ is considered. This is the mode-mode coupling approximation which has been used in the theory of liquids[14] and of anharmonic solids.[13]

(2) The projection operator Q is neglected in the time development of the product states (i.e., the states at a later time are taken as orthogonal to the original variables):

$$(z - Q\mathcal{L}Q)^{-1} \rightarrow (z - \mathcal{L})^{-1}.$$ (53)

This approximation is always made in the derivation of the Fokker-Planck equations.[12]

(3) The time development of the product states is factorized, i.e., we always assume that

$$\langle A_i A_j| e^{-i\mathcal{L}t}A_k A_l\rangle = \beta^{-1}(\langle A_i| e^{-i\mathcal{L}t}A_k\rangle\langle A_j| e^{-i\mathcal{L}t}A_l\rangle + \langle A_i| e^{-i\mathcal{L}t}A_l\rangle\langle A_j| e^{-i\mathcal{L}t}A_k\rangle).$$ (54)

With these approximations, the explicit term of the imaginary part of M_{22} is derived in the Appendix. We get

$$M''_{22}(\omega_1, (k+G_1)_x, (k+G_2)_x)$$

$$= -\frac{k_B T A^2 \pi}{16 M^B c^2 a^3 B^3} \sum_{\vec{G}',\vec{G}''} e^{-(\vec{G}'^2+\vec{G}''^2)/4B}$$

$$\times \int_{-q_m}^{q_m} dq_x(q-G')_x(q-G'')_x \exp[q_x(G'+G'')_x/(2B)]$$

$$\times \int_{cq_x}^{\omega_D} d\omega\, \omega^{-1} e^{-\omega^2/2Bc^2}\{[(\omega/c)^2 + \vec{G}'\cdot\vec{G}'' - q_x(G'+G'')_x]I_0(x) - 2Bx I_1(x)\}$$

$$\times [\Phi''_{11}(\omega+\omega_1, (k+q+G'+G_1)_x, (k+q+G''+G_2)_x)+\Phi''_{11}(\omega \rightarrow -\omega)],$$ (55)

where $x = [(\omega/c)^2 - q_x^2]^{1/2}(\vec{G}'+\vec{G}'')_\perp/2B$. G'_x is the x component and $G'_\perp$ is the normal component of the reciprocal-lattice vector $\vec{G}'$. q_m is the maximum wave vector of the Debye spectrum and ω_D is the Debye frequency. I_0 and I_1 are Bessel functions which result from the angular integration over $\vec{q}$. The real part of M_{22} can be obtained by Kramers-Kronig transformation.

Equation (55) is the final equation of this section. It allows an explicit evaluation of M_{22}. However, we have to note that it involves Φ''_{11}. To calculate Φ''_{11} from Eq. (22) we need to know M_{22}; i.e., (55) has to be solved iteratively.

The main approximation in the above procedure is the neglect of the term $|Q(\mathcal{L}e^{ikx})p\rangle$ compared to the term $|Q(\mathcal{L}p)e^{ikx}\rangle$ in the calculation of the memory function (52). Evaluating the time derivatives one finds for the ratio of neglected to considered terms for the memory function, roughly (with the parameters used in the figures)

$$N^{-1} \sum_{\vec{q},\alpha} \left\langle \left[\partial V^{(1)}\left(x, \begin{pmatrix}\vec{q}\\\alpha\end{pmatrix}\right)/\partial x\tilde{Q}\begin{pmatrix}\vec{q}\\\alpha\end{pmatrix}\right]^2\right\rangle \frac{(k/M^A)^2\langle p^2|Qp^2\rangle}{}$$

$$\approx 10^{-3}\frac{k^2 a^2 k_B T M^B c^2}{\Delta E^2}$$

$$\approx 10^{-2} a^2 k^2 (k_B T/\Delta E)^2.$$ (56)

This means that our approximations hold true as long as $k_B T$ is substantially smaller than ΔE (ak is in general not small compared to one because of the presence of umklapp processes).

E. Fokker-Planck limit for M

It is interesting to compare (55) with the result obtained in the Fokker-Planck limit. We follow the procedure suggested by Forster[12] and apply the same approximations to the memory kernel. Let us first write the Liouvillian as

$$\mathcal{L} = \mathcal{L}^A + \mathcal{L}^B + \mathcal{L}^{B \to A} , \tag{57}$$

where

$$\mathcal{L} = -i \frac{p}{M^A} \frac{\partial}{\partial x} \tag{58}$$

represents a freely propagating particle A,

$$\mathcal{L}^B = -i \sum_{l,\alpha} \frac{p_\alpha(l)}{M^B} \frac{\partial}{\partial u_\alpha(l)} + \frac{i}{2} \sum_{l_1,l_2;\alpha_1,\alpha_2} \Phi^{(2)}_{\alpha_1 \alpha_2}(l_1, l_2) u_{\alpha_1}(l_1) \frac{\partial}{\partial p_{\alpha_2}(l_2)} + i \sum_{l,\alpha} V^{(1)}(x, l) \frac{\partial}{\partial p_\alpha(l)} \tag{59}$$

is the part of the Liouvillian that acts only on the coordinates of the lattice particles, and

$$\mathcal{L}^{B \to A} = i \sum_l \left(\frac{\partial V}{\partial x} + \sum_\alpha \frac{\partial V^{(1)}(x, l)}{\partial x} u_\alpha(l) \right) \frac{\partial}{\partial p} \tag{60}$$

represents the influence of the lattice on the mobile particle. Then one can show that the vertex $|Q\mathcal{L}p\rangle$ in (25) becomes

$$|Q\mathcal{L}p((k+G_2)_x)\rangle = |Q\mathcal{L}^{B \to A}p((k+G_2)_x)\rangle$$

$$= i \left| Q\left[\sum_l \left(\frac{\partial V}{\partial x} + \sum_\alpha \frac{\partial V^{(1)}(x, l)}{\partial x} u_\alpha(l) \right) e^{i(k+G_2)_x x} \right] \right\rangle = i|QF e^{i(k+G_2)_x x}\rangle , \tag{61}$$

where F is the force on the mobile particle. The Fokker-Planck limit is then obtained by

(1) replacing $Q\mathcal{L}Q$ by $\mathcal{L}^B$ (valid for $M^A/M^B \to \infty$)
(2) decoupling force from density fluctuations,
and
(3) white-noise approximation to forces.

Then

$$M^{FP}_{22}(z, (k+G_1)_x, (k+G_2)_x) = -\langle e^{i(k+G_1)_x x} FQ|(z-\mathcal{L}_0)^{-1}QF e^{i(k+G_2)_x x}\rangle ,$$

$$= -\beta^{-1}\langle e^{i(k+G_1)_x x} | e^{i(k+G_2)_x x}\rangle\langle FQ|(z-\mathcal{L}_0)^{-1}QF\rangle = M^B \gamma d(G_{2x} - G_{1x}) . \tag{62}$$

The same result is obtained by using the backward Fokker-Planck operator instead of the Liouvillian in (22)–(25). Then the damping term (62) arises directly from the momentum-momentum matrix element of Ω (which now does not vanish); i.e., in the Fokker-Planck formulation the damping is already included in the frequency matrix and arises because the Fokker-Planck operator is not Hermitian.[12]

Note that in the Fokker-Planck approximation one gets

$$M(z)\chi^{-1} = M_{22}(z)\chi_{22}^{-1} = M^B/M^A \gamma \delta(G_{1x}, G_{2x}) , \tag{63}$$

i.e., the damping term in (22) becomes diagonal in the reciprocal-lattice vectors and independent of them (i.e., spatially independent), independent of z (i.e., frequency independent), and vanishes for $M^B/M^A \to 0$.

The advantages of (55) over (63) are then:

(1) The frequency and spatial dependence of the damping can be taken into account, at least approximately.

(2) The absolute value of the damping (at least the

contribution from the decay of a density fluctuation into another density fluctuation and a phonon) can be calculated. In particular one can study the influences of different diffusing and host masses, different elastic constants, and the temperature dependence of γ.

F. Relation to experimental quantities

Since we are calculating only self-correlation functions of the diffusing particle, we can only calculate incoherent or one-particle properties of the diffusion. That is, strictly speaking we can only find the tracer diffusion constant and the incoherent neutron scattering cross section. However, we will also give a one-particle approximation to the frequency-dependent conductivity $\sigma(\omega)$. When comparing this with experiment, one always has to bear in mind that all correlation effects and all contributions from the lattice are neglected.

(α) *Incoherent neutron scattering.* The incoherent neutron scattering cross section is proportional to the incoherent scattering law $S_s(k, \omega)$, which is given by (classically)

$$S_S(k, \omega) = -2\beta^{-1}\Phi_{11}''(z, k, k) = \lim_{\eta \to 0} (-2/\beta) \operatorname{Im}[\chi_{11}/z + \Omega_{12}\chi_{22}^{-1}/z^2(z + M_{22}\chi^{-1} - \Omega_{21}\chi_{11}^{-1}z^{-1}\Omega_{12}\chi_{22}^{-1})^{-1}\Omega_{21}]. \tag{64}$$

For $k = 0$ the second term in (64) vanishes because both Ω_{12} and Ω_{21} contain a factor k, therefore we are left with $-2\chi_{11}/\beta z = 2\pi k_B T \delta(\omega)$, i.e., a δ function at the origin. There is no admixture from higher reciprocal-lattice vectors. As k increases, these higher terms gain in intensity $\sim k^2$, while the peak at $\omega = 0$ develops a finite width.

(β) *Tracer diffusion constant.* The tracer diffusion constant is given by the $\omega = 0$ limit of the Fourier transform of the velocity-velocity correlation function and can hence be expressed as

$$D = \lim_{\omega \to 0} \left(-\frac{1}{\beta(M^A)^2}\Phi_{22}''(z, 0, 0) \right) = \lim_{\omega \to 0}\lim_{k \to 0} \left(\frac{-\omega^2}{\beta k^2}\Phi_{11}''(z, k, k) \right)$$

$$= \lim_{\omega \to 0}\lim_{k \to 0} \left(-\frac{1}{\beta(M^A)^2} \right) \operatorname{Im}[(z + M_{22}\chi_{22}^{-1} - \Omega_{21}\chi_{11}^{-1}z^{-1}\Omega_{12}\chi_{22}^{-1})^{-1}\chi_{22}], \tag{65}$$

where the $G_1 = G_2 = 0$ element of the matrix Φ_{22}'' has to be taken.

(γ) *Frequency-dependent conductivity* $\sigma(\omega)$. As we have already noted this is really a coherent property of the crystal, but here we give the single-particle contribution of the diffusing ion to $\sigma(\omega)$. This is also related to the velocity-velocity correlation function and is given by

$$\sigma(\omega) = -\frac{ne^2}{(M^A)^2}\Phi_{22}''(z, 0, 0), \tag{66}$$

where we wrote σ to emphasize that it is a single-particle contribution. n is the number of diffusing particles per unit volume and e their charge. Note that

$$\sigma(0) = \beta ne^2 D, \tag{67}$$

which is just the Nernst-Einstein relation in the absence of correlation.

III. DETAILS OF THE CALCULATION

In order to get the experimental quantities in which we are interested, we have to solve Eq. (55). This is an integral equation involving a double integration at each step. This problem can in principle be solved iteratively, but would be very time consuming on the computer. So as a first approximation to M_{22} we take only the first iteration of (55), i.e., we approximate Φ_{11}'' by the results obtained in the absence of M_{22}. This means that we approximate broad modes by δ functions. As long as the widths of these modes are smaller than the structure in the integration kernel and the range of the integration, we expect to get at least qualitatively correct results by this approximation. The difficulties arising from this approximation will be discussed when they occur in the next section. The real part of M_{22} is neglected altogether since it only leads to a shift of the features observed, but does not change them qualitatively.

A. "Dispersion curves"

If M_{22} is neglected in the calculation of Φ_{11} then Φ_{11} has an imaginary part only at frequencies which are the square roots of the eigenvalues of $\Omega_{21}\chi_{11}^{-1}\Omega_{12}\chi_{22}^{-1}$, as may be seen by inspection of (64). Clearly these dispersion curves do not represent the true dispersion of our system because M_{22} is not small. Moreover they depend sensitively on the particular choice for the variable considered explicitly. Nevertheless, we will find them useful later in the discussion of various properties of the correlation functions.

In the limit $M_{22} = i\eta \to 0$, the integral over ω in (55) is replaced by a discrete sum over δ functions with weights determined by the full (64) at the square roots of the eigenvalues as long as these are in the interval of the integration. It is therefore of interest to see explicitly what these frequencies are. To do this we first of all write

$$\Omega_{21}\chi_{11}^{-1}\Omega_{12}\chi_{22}^{-1} = \sum_{G_x'} (k + G')_x d(G_{1x} - G_x')$$

$$\times d^{-1}(G_x' - G_{2x})(k + G_2)_x k_B T/M^A. \tag{68}$$

In the limit of high temperatures, d is diagonal. The off-diagonal terms vanish approximately as $\Delta E/k_B T$, where ΔE is the energy difference between maximum and minimum in Fig. 1. Then (68) becomes

$$\Omega_{21}\chi_{11}^{-1}\Omega_{12}\chi_{22}^{-1} \simeq (k + G_1)_x^2 k_B T/M^A \delta(G_{1x}, G_{2x}), \tag{69}$$

i.e., the frequencies just become

$$\omega = \pm |(k + G_1)_x| (k_B T/M^A)^{1/2}, \tag{70}$$

i.e., we get a straight dispersion with a slope $\sim (T/M^A)^{1/2}$. Nondiagonal d leads to a mixing of modes originating from different values of G_1, which affects the modes most at the zone boundary where they are degenerate in the absence of
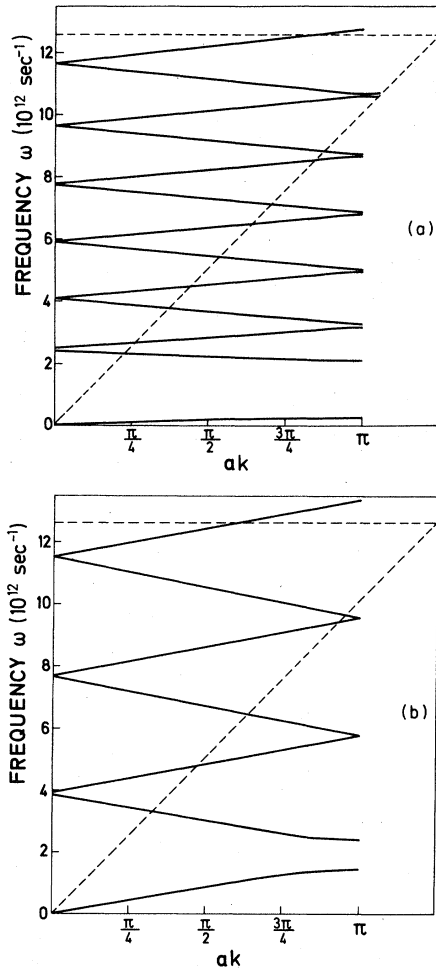
FIG. 2. Dispersion curves for density fluctuations for $M_{22} = 0$ with $A = 2000$ K, $B = 5/a^2$, $a = 3$Å, $c = 10^5$ cm/sec, $M^A = M^B = 50$ amu: (a) $T = 50$ K, (b) $T = 200$ K.

this mixing, and leads to a splitting. At finite temperatures we can write with the aid of (38),

$$\Omega_{21}\chi_{11}^{-1}\Omega_{12}\chi_{22}^{-1}(G_{1x}, G_{2x}) = (k + G_1)_x^2 k_B T / M^A \delta(G_{1x}, G_{2x})$$

$$\times i/M^A K(G_{1x} - G_{2x})(k + G_2)_x .$$

(71)

This shows that as $T \to 0$ the diagonal term vanishes, whereas the terms depending explicitly on the effective potential remain finite and are proportional to $(M^A)^{-1/2}$ in the frequency.

In Fig. 2 we show the dispersion curves calculated explicitly with the full $d(G)$ for the potential corresponding to $c = 10^5$cm/sec in Fig. 1 (activation energy 200 K) for $T = 50$ K (a) and 200 K (b). The results suggested by (70) and (71) are borne out qualitatively. The slopes of the dispersion curves at 300 K are greater than the 50 K ones, as suggested by (70). In fact for the

higher branches the ratio of the slopes is exactly 2, as predicted by (70). At the zone boundary there is a gap which is relatively larger in the 50-K case, a manifestation of the greater importance of the off-diagonal coupling terms in $d(G)$. If the temperature is increased beyond 200 K, the form predicted by (70) is approximated more and more closely. The first gap at the zone boundary is determined largely by $d(1)$, the second gap by $d(2)$, etc. However, $d(1) > d(2) > d(3)$, etc., explaining why the higher gaps are smaller. In the 50-K case the first gap at $k = 0$ is larger than the higher ones (2.4 instead of 1.8×10^{12} sec^{-1}). In fact, as the temperature is decreased further, the higher gaps decrease $\sim \sqrt{T}$, whereas the lowest one approaches asymptotically a limiting frequency of 2.35×10^{12} sec^{-1}. This has to be compared to the Einstein oscillator frequency of 2.48×10^{12} sec^{-1} in this case and shows clearly that this limiting behavior is a consequence of the off-diagonal term in (71). The discrepancy between our limiting frequency and the Einstein oscillator frequency is explained by bearing in mind that $K(G)$ in (71) samples the whole potential, not just the curvature at the bottom of the potential. The average curvature of the potential, however, is lower, due to the bending down of the potential at the top (Fig. 1). This leads to our lower "effective Einstein frequency."

As the temperature decreases, the lowest dispersion curves become much flatter than predicted by (70), emphasizing again their Einstein-type character. The range of the integration as given by (55) is indicated by the dashed triangle in Fig. 2. Only branches within the triangle contribute (for $\omega_1 = 0$; for $\omega_1 \neq 0$ the triangle is shifted and split).

B. $k = 0$ and $\omega_1 = 0$ limit

The expression (55) for

$$M_{22}(\omega_1, (k + G_1)_x, (k + G_2)_x)$$

contains a factor ω^{-1}, which can lead to a divergent contribution for $q_x \to 0$, so special care has to be taken. However, for the first iteration Φ_{11}'' consists of a series of δ functions in ω; therefore difficulties only arise if $\omega = 0, q = 0$ coincides with one of the δ-function peaks of

$$\phi_{11}''(\pm\omega + \omega_1, (k + q + G' + G_1)_x, (k + q + G'' + G_2)_x),$$

i.e., most notably at $\omega_1 \to 0$ and $k \to 0$. We treat this case specifically by setting $k = 0$ and considering the $\omega_1 \to 0$ limit. Then by inspection of the dispersion curves in Fig. 2 we see that a section of the lowest dispersion branch of length $\sim \omega_1$

contributes, and that the factor $1/\omega$ becomes approximately $1/\omega_1$, i.e., the frequency factors cancel and we get a finite contribution from the lowest branch, even in the limit $\omega_1 \to 0$. We are now going to work this out analytically.

First we bear in mind that there is a contribution only if ω_1, ω, and q are small ($k = 0$). Then in (55), $x \to 0$ and by replacing all terms by their limits the corresponding contribution M_{220} to M_{22} becomes

$$M''_{220}(\omega_1 \to 0, G_{1x}, G_{2x}) = -\frac{\pi k_B T A^2}{16 M^B c^2 a^3 B^2} \sum_{\vec{G}',\vec{G}''} e^{-(\vec{G}'^2 + \vec{G}''^2)/(4B)} (\vec{G}' \cdot \vec{G}'')^2$$

$$\times \int_{-q_m}^{q_m} dq_x \int_{c|q_x|}^{\omega_D} d\omega\, \omega^{-1} [\Phi''_{11}(\omega + \omega_1, (q + G' + G_1)_x, (q + G'' + G_2)_x)$$

$$+ \Phi''_{11}(\omega \to -\omega)] . \tag{72}$$

Φ''_{11} are δ functions and in Fig. 2 we see that for small q and ω the lowest branch may be approximated by

$$\Phi''_{11}(\omega + \omega_1, (q + G' + G_1)_x, (q + G'' + G_2)_x) \simeq \delta(\omega + \omega_1 - c_0 q_x) \Psi_{11}((G' + G_1)_x, (G'' + G_2)_x), \tag{73}$$

where Ψ_{11} is a matrix of weight functions, c_0 is the slope of the lowest dispersion branch, and $c_0 < c$ is assumed. The integrals in (72) can then be evaluated to give

$$M_{220}(\omega_1 \to 0, G_{1x}, G_{2x}) = -\frac{k_B T \pi A^2}{16 M^B c^2 a^3 B^3} \sum_{\vec{G}',\vec{G}''} e^{-(\vec{G}'^2 + \vec{G}''^2)/4B}$$

$$\times (\vec{G}' \cdot \vec{G}'')^2 \Psi_{11}((G' + G_1)_x, (G'' + G_2)_x) c_0^{-1} \ln[(c + c_0)/(c - c_0)] . \tag{74}$$

This expression is independent of ω_1 as we had expected. In practical calculations this expression was used for $\omega_1 = 0$ and including it led to a good agreement of the calculations for $\omega_1 = 0$ and ω_1 small but finite (where the lowest branch is already included in the integral and does not have to be added on artificially).

IV. RESULTS

In this section we discuss the results of our explicit numerical calculations. As far as possible we give physical or mathematical reasons for their qualitative behavior. Whenever possible we compare these results with what would be expected in a simple Fokker-Planck (FP) model (in the large-friction limit). In Sec. IV.A. we show some of the general features of M_{22}, while in the later sections we discuss their implications for the diffusion constant, the frequency-dependent conductivity $\sigma(\omega)$ in the one-particle model, and finally $\Phi_{22}(q, \omega)$ and $\Phi_{11}(q, \omega)$. For $\Phi_{11}(q, \omega)$ we compare our results also with the Chudley-Elliott model.

A. $\tilde{M}_{22}$

We have seen in Sec. II that in a simple FP model $\tilde{M}_{22}$ should be diagonal in the reciprocal-lattice vectors G_1 and G_2 and independent of these and the wave vector $\vec{k}$. However, from general principles one would expect that $\tilde{M}_{22} \to 0$ as the wave vectors become very large, since very-short-wavelength functions cannot be damped.

In Fig. 3 we show the calculated wave-vector dependence of the diagonal element $\tilde{M}''_{22}(\omega_1 = 0, k, k)$ (which is constant in the FP limit) and the off-diagonal terms $\tilde{M}''_{22}(\omega_1 = 0, k, k + 2\pi/a)$ and $\tilde{M}''_{22}(\omega_1 = 0, k, k + 4\pi/a)$ (which vanish in the FP limit). First of all, we notice that all three matrix elements decrease around $k = 6\pi/a$ (for our particular set of parameters), corresponding to three reciprocal-lattice vectors. This is in agreement with what we had expected and can be understood by inspection of the dispersion curves in Fig. 2(b), which are calculated for the same
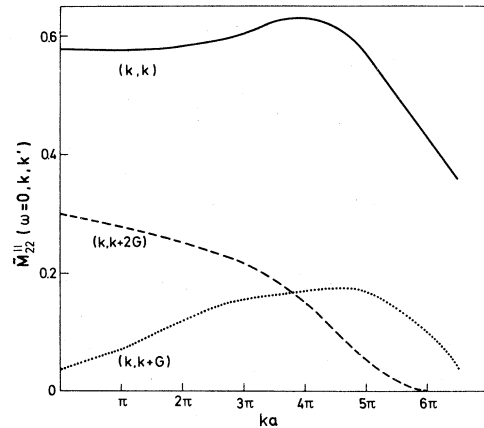
FIG. 3. Momentum dependence of the imaginary part of the memory kernel for $\omega = 0$ in units of 10^{12} sec^{-1} with $A = 2000$ K, $B = 5/a^2$, $a = 3$Å, $c = 10^5$ cm/sec, $M^A = M^B = 50$ amu, $T = 200$ K.

set of parameters. One sees that the dispersion curves from three reciprocal-lattice vectors fit into the dashed interval of integration. Since higher branches can contribute only via the off-diagonal elements in $d(G)$ [which are much smaller than $d(0)$], this explains the decrease of M_{22}. This observation leads to a general rule, since the slopes of the dispersion curves are $\sim(T/M^A)^{1/2}$ and the interval of integration approximately equals the sound velocity c in the host lattice, i.e., $\sim(c_E/M^B)^{1/2}$, where c_E is the effective elastic constant and M^B the mass of the host atoms. We find that the wave vector k_c at which M_{22} decreases is

$$k_c \approx \frac{M^A}{M^B}\frac{c_E}{T},\tag{75}$$

i.e., departures from the Fokker-Planck limit are particularly important for small M^A/M^B, i.e., light diffusing masses. This is just what is expected from the derivation of the FP equations, where $M^A/M^B \gg 1$ was assumed. Furthermore, we see that the off-diagonal matrix elements in M_{22} may be as large as 50% of the diagonal ones and therefore cannot be neglected.

The situation with respect to the frequency dependence of $\tilde{M}_{22}$ is similar. In the FP approximation one assumes that the forces exerted by the lattice are completely uncorrelated in time, i.e., that the damping is independent of frequency. However, one expects that for very short times the particles do not collide and therefore move undamped. Therefore we expect that $\tilde{M}_{22}''(\omega) \to 0$ as $\omega \to \infty$. In Fig. 4 we plot
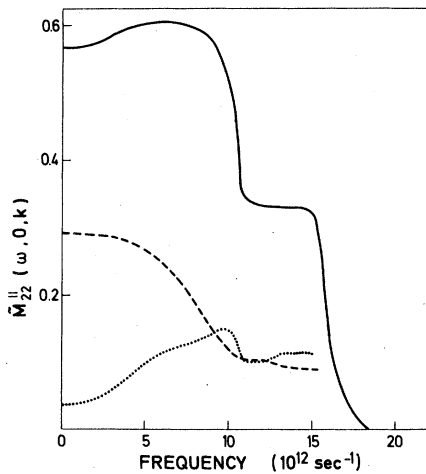
FIG. 4. Frequency dependence of the imaginary part of the memory kernel in units of 10^{12} sec^{-1} for three different momenta: — $ak=0$, --- $ak=2\pi$, $\cdots$ $ak=4\pi$ with $A=2000$ K, $B=5/a^2$, $a=3$Å, $c=10^5$ cm/sec, $M^A =M^B=50$ amu, $T=200$ K.

$\tilde{M}_{22}''(\omega, k=0, k=0)$, $M_{22}''(\omega, k=0, k=2\pi/a)$, and $\tilde{M}_{22}''(\omega, k=0, k=4\pi/a)$. All three show a decrease near $\omega = \omega_D$. The mathematical reason for this behavior is that at $\omega > \omega_D + \omega_0$ (ω_0 is the lowest nonvanishing frequency of a dispersion branch at $k=0$) there is no direct overlap between the shifted first dispersion branch in (56) and the interval of integration. The main decrease of $\tilde{M}_{22}''(\omega)$ occurs in the range $\omega_D - \omega_0 < \omega < \omega_D + \omega_0$, i.e., at high temperatures the decrease is smoother than at low temperatures (the interval is $\sim \sqrt{T}$ at high temperatures). It is physically plausible that the decrease is centered around ω_D, since this just means that the correlation time for the forces exerted by the lattice is a typical period of vibrations of the lattice ions.

The discontinuous decrease of $\tilde{M}_{22}''$ in Fig. 4 is a consequence of the δ-function approximation to Φ_{11}, since that means that a point of the dispersion curve either contributes completely or not at all to the integral, whereas a finite width would smooth the dependence, effectively convoluting the calculated behavior by the widths of the lines (typically $1-5 \times 10^{12}$ sec^{-1}).

The frequency dependence of $\tilde{M}_{22}''$ is important in the calculation of the frequency dependence of, for example, $\sigma(\omega)$ if $\omega_D \sim \omega_0$ [since the structure of $\sigma(\omega)$ occurs at ω_0]. Since $\omega_D \sim 1/(M^B)^{1/2}$ and $\omega_0 \sim M^A$, we again see that the departures from the constancy of $\tilde{M}_{22}''(\omega)$ are particularly important for $M^A/M^B \ll 1$.

These considerations also impose limits on the parameter values which can be treated within our approximation. We expect to get sensible results only if at least one dispersion branch is included completely in the frequency interval of integration and if the total number of dispersion curves considered (we could treat a maximum of 15 in a reasonable computer time) spans a frequency interval somewhat greater than ω_D. This leads to the following approximate condition:

$$4 \lesssim T/M^A c \lesssim 40,\tag{76}$$

where T is measured in K, M^A in amu, and the sound velocity c of the host in 10^5 cm/sec. By making the treatment self-consistent it would be possible to relax the upper limit by including more reciprocal lattice vectors in the lower limit. The number of reciprocal-lattice vectors also leads to another condition via the convergence of $d^{-1}(G)$ [Eq. (32)]:

$$\Delta E/T \lesssim 8,\tag{77}$$

where ΔE is the activation energy for the mobile ion.
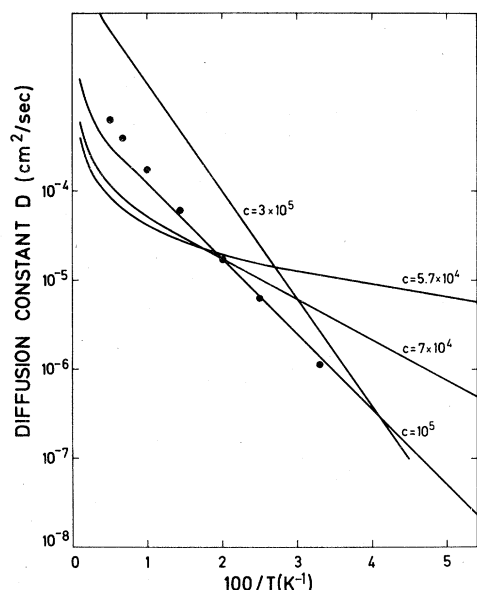
FIG. 5. Diffusion constant as function of temperature for various sound velocities (cm/sec) with $A = 2000$ K, $B = 5/a^2$, $a = 3$Å, $M^A = M^B = 50$ amu. The solid lines are calculated with a constant M_{22} chosen to lead the same diffusion constant as the full M_{22} at $T = 50$ K. The points have been calculated for $c = 10^5$ cm/sec using the full M_{22}.

B. Diffusion constant D

The general expression for D is given in Eq. (65). In a zeroth-order approximation one may use the Fokker-Planck approximation for M, i.e., M approximated by an effective damping constant γ. Evaluation of Eq. (65) shows then that D is in a good approximation inversely proportional to γ. If one assumes $\gamma \sim (M^A)^{-1}$ [as one might expect from the χ_{22}^{-1} factor in (22)], but independent of T, M^B, and c, then one gets a diffusion constant which is independent of M^A, M^B, and c, and, at low T, depends on temperature with a simple Arrhenius law. The activation en-

TABLE I. Activation energy ΔE and frequency ω_0 of the reststrahlen oscillator as function of the elastic constant c, calculated from the fully relaxed periodic potential, using $A = 2000$ K, $B = 5/a^2$, $a = 3$ Å, $M^A = 50$ amu.

c (10^5 cm/sec)	ΔE (K)	ω_0 (10^{12} sec^{-1})
0.57	27.4	2.22
0.7	109.7	1.31
0.8	151.8	1.93
1.0	201.2	2.47
1.2	228.0	2.72
3.0	279.0	3.14

ergy is exactly the barrier height in Fig. 1, i.e., it decreases with decreasing c. This behavior is demonstrated clearly in Fig. 5, where we show the temperature dependence of D for the potential shown in Fig. 1 using the approximation (63) for M. The corresponding heights of potential barriers are given in Table I. The damping γ was chosen so that the curves agree with the results using the full M_{22} at $T = 50$ K. At high T (where the neglect of higher powers in the momenta however, is less justified), $D(T) \sim T$, $\sigma(\omega = 0, T)$ → constant [i.e., the corresponding plots for $\sigma(\omega = 0, T)$ would curve down rather than up for high T, in agreement with experiment[1,2]].

The advantage of our treatment is that we can calculate the absolute value and dependence on T, M^A, M^B, and c of the damping (matrix) explicitly. Therefore we do not have to resort to the *ad hoc* assumptions of the Fokker-Planck treatment. We are now going to study the dependence on the various parameters in turn.

In Table II we give as an example the temperature dependence of selected elements of the memory matrix for $M^A = 5$ amu. First of all we note that the matrix elements decrease with increasing wave vector and that this decrease occurs at smaller wave vectors if the temperature is higher,

TABLE II. Temperature dependence of various matrix elements of $\tilde{M}_{22}$ for the parameters $A = 2000$ K, $B = 5/a^2$, $a = 3$ Å, $c = 10^5$ cm/sec, $M^A = 5$ amu, $M^B = 50$ amu, $\omega = 0$. M_{22} is given in units of 10^{12} sec^{-1}.

T (K)	30	40	50	70	100	150	200
$\tilde{M}_{22}''(0,0)$	6.02	6.18	6.12	5.88	5.48	4.78	4.15
$\tilde{M}_{22}''(2\pi/a, 2\pi/a)$	8.75	7.51	6.65	5.39	4.23	3.53	3.63
$\tilde{M}_{22}''(4\pi/a, 4\pi/a)$	3.17	3.13	3.71	3.83	2.87	1.30	0.63
$\tilde{M}_{22}''(6\pi/a, 6\pi/a)$	4.24	1.71	0.24	-0.30	-0.16	-0.03	-0.01
$\tilde{M}_{22}''(0, 2\pi/a)$	1.90	1.32	1.04	0.72	0.47	0.45	0.63
$\tilde{M}_{22}''(0, 4\pi/a)$	2.06	2.60	2.87	2.80	2.12	1.27	0.83

in agreement with (75). Furthermore, we also note that the matrix elements generally decrease with increasing T [this arises from the smaller $1/\omega$ factors in (55) for the steeper dispersion curves at high T]. Since the diffusion constant is approximately proportional to M_{22}^{-1} (it is no longer exact, since there are off-diagonal matrix elements), D increases more rapidly with T than $e^{-\Delta E/k_B T}$. For the case $M_A = 5$ amu and $c = 10^5$ cm/sec, the resulting diffusion constants are shown as crosses in Fig. 5. One can see that the temperature dependence is still approximately exponential, but not precisely; i.e., if one forces the functional form to be exponential, then the apparent activation energy is temperature dependent. For very low T, $\Delta E^{\text{eff}}(T) \rightarrow \Delta E$, the FP value, whereas for higher T, $\Delta^{\text{eff}}(T) > \Delta E$.

In Table III we show the dependence of ΔE^{eff} (determined between $T_1 = \frac{1}{2}\Delta E$ and $T_2 = \frac{1}{4}\Delta E$) and ν on M_A [$D = \nu \exp(-\Delta E^{\text{eff}}/k_B T)$]. It shows clearly that the additional temperature dependence from the memory matrix leads to a stronger temperature dependence than in the FP case ($\Delta E = 200$ K) and that this departure becomes more dramatic for lighter diffusing ions. For light diffusing ions the prefactor varies approximately as $1/(M^A)^{1/2}$, whereas for heavy diffusing masses, D is almost independent of M^A. Both these results are contrary to what is expected from classical rate theory which predicts a prefactor $1/(M^A)^{1/2}$ and a mass-independent activation energy for all diffusing masses. Physically, this departure from the classical rate theory can be understood by bearing in mind that in the classical theory one assumes that the lattice is always in equilibrium with the diffusion ion, i.e., fully relaxed. If the diffusing particle, however, is very light, then the lattice particles cannot always follow the diffusing ion to their momentary equilibrium positions, i.e., the lattice is not fully relaxed, leading to a higher apparent activation energy. This effect will be most pronounced for small M^A/M^B.

As far as we know, this is the first time that a dependence of the activation energy on the mass of the diffusing particle has been predicted in a classical theory. The mass dependence is in qualitative agreement with that found experimentally for hydrogen isotopes in fcc metals.[2] The standard explanation for this behavior is in terms of the quantum theory of diffusion,[2] but our calculations show that it might be possible to explain the experimental results without having to invoke quantum theory, whose applicability appears questionable at the high temperatures and comparatively high masses encountered in hydrogen diffusion. In the classical rate theory the prefactor of the exponential is given by

$$\nu = \nu_0 a^2, \qquad (78)$$

where ν_0 is the Einstein frequency of the defect and a the jump length, i.e., the lattice constant. Using our potential we predict for $M^A = 5$, that $\nu = 10.5$ compared to the value 15.1 in Table II; i.e., we predict an attempt frequency about 50% larger than in the classical case. However, if one repeats the fit for $T_1 = 40$ K and $T_2 = 30$ K, one gets $A = 9.5$ and $\Delta E^{\text{eff}} = 202$ K, in rather closer agreement with the classical result and with our previous observation that ΔE^{eff} decreases with decreasing T. In fact this is a prediction of our theory which has not yet been checked experimentally, but should provide a useful test for its validity. Similarly we investigated the influence of the mass of the host atoms on the effective activation energy and the prefactor. The results are summarized in Table IV. We find that the activation energy increases with increasing M^B, which emphasizes again the point that the ratio M^B/M^A is the important quantity for determining the departure from the FP behavior. The decrease in the prefactor can be understood by bearing in mind that $c \sim 1/(M^B)^{1/2}$ for fixed elastic constants. Therefore the density of phonon states into which a diffusion mode can decay increases with M^B and the damping for the diffusion mode therefore also increases; D therefore

TABLE III. Effective activation energy ΔE^{eff} (in K) and prefactor ν (in 10^{-4} cm²/sec) for the diffusion constant $D(T)$ for $T_1 = 100$ K and $T_2 = 50$ K as a function of M^A. Other parameters as in Table II.

M^A	ν	ΔE^{eff}
3	18.5	225
5	15.1	224
7	12.8	215
10	12.2	213
20	12.0	213
40	11.3	213

TABLE IV. Effective activation energy ΔE^{eff} (in K) and prefactor ν (in 10^{-4} cm²/sec) for the diffusion constant $D(T)$ for $T_1 = 100$ K and $T_2 = 50$ K as a function of the host atom mass M^B. $M^A = 20$ amu, other parameters as in Table II.

M^B	ν	ΔE^{eff}
50	12.0	213
100	8.7	214
150	8.0	221
250	6.9	221

decreases. At a given temperature, D varies roughly as $1/(M^B)^{1/2}$.

If the elastic constant decreases, then the sound velocity c also decreases and with it the barrier height as shown in Fig. 1 and Table I. Thus the temperature dependence of the diffusion constant becomes less rapid. Also with decreasing c the phonon density of states increases and decays of the diffusion mode become more likely [there is a factor $1/c^2$ in (55)]; this leads to an increased damping for small c and hence a smaller prefactor ν.

C. Frequency-dependent conductivity σ (ω)

As we have seen in Eq. (66) the frequency-dependent conductivity (in the single-particle approximation) σ (ω) is simply related to $\Phi_{22}(\omega, k = 0, k = 0)$. If $M''_{22}(\omega, k = 0, k = 0)$ is known, it is a simple matter to calculate it.

In Fig. 6 we show σ (ω) in arbitrary units for four different temperatures. It shows that σ (0) $\neq 0$ for all temperatures, corresponding to the finite dc conductivity of our model (related to the finite diffusion constant D). Generally speaking, σ (ω) shows a two-peak structure, one peak centered at $\omega = 0$ and one at a finite frequency. The peaks arise from the dispersion branches at $k = 0$ (compare Fig. 2). Only the lowest two branches contribute noticeably to σ (ω), since one is considering the $k = 0$ limit. Higher branches are associated with higher reciprocal-lattice vectors which couple only via small $d(G)$'s and therefore have a low weight associated with them (there are small indications of a third peak in the $T = 30$
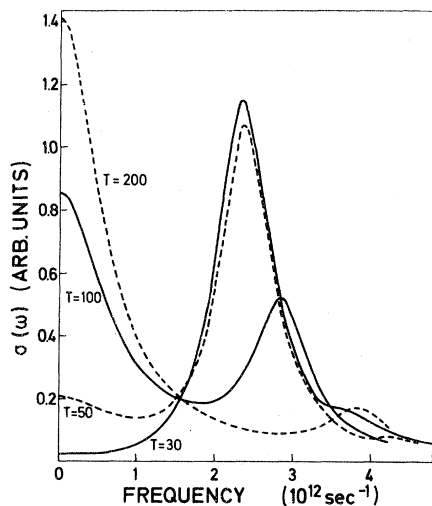
FIG. 6. Conductivity as function of frequency for four different temperatures with $A = 2000$ K, $B = 5/a^2$, $a = 3$Å, $c = 10^5$ cm/sec, $M^A = M^B = 50$ amu.
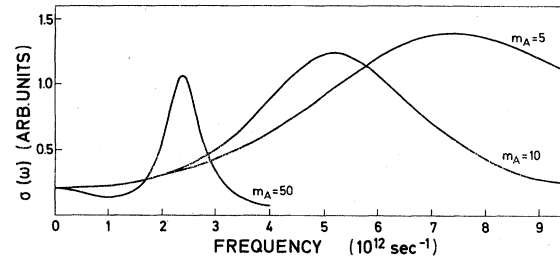
FIG. 7. Conductivity as function of the frequency for different masses for the diffusing particle with $A = 2000$ K, $B = 5/a^2$, $a = 3$Å, $c = 10^5$ cm/sec, $M^B = 50$ amu, $T = 50$ K.

and $T = 50$ curves around $\omega = 4 \times 10^{12}$ sec^{-1}). As we have seen, the mode at finite frequency shifts to lower frequency as T decreases and approaches the Einstein oscillator frequency for low T (in Fig. 6 there is hardly any shift in the peak between $T = 50$ K and $T = 30$ K). The most dramatic feature of Fig. 6 is the gradual shift of weight from the Einstein oscillator peak to the diffusion peak at $\omega = 0$ as T increases. The mathematical reason is the decrease of $d(G)$ with increasing T. Physically this behavior is very reasonable, too. At low temperatures the particle is mainly localized in one of the potential minima and oscillates around it, therefore the oscillatory peak is dominant. At high temperatures, on the other hand, the particle is moving fairly often above the maxima of the potential and the diffusive peak is bigger. The total area under the curve is independent of T (and M^B and c, for that matter), a consequence of the sum rule

$$\int_0^\infty d\omega\, \sigma\ (\omega) = \frac{n\pi(Ze)^2}{2M^A}. \tag{79}$$

Figure 7 shows the dependence of σ (ω) on the mass of the diffusing particle (for $T = 50$ K). The features worth noting are that σ (0) depends only very little on M^A (the differences are a few percent and do not show up at all in Fig. 7), contrary to the $1/(M^A)^{1/2}$ dependence predicted by classical theory. The frequency of the Einstein oscillator peak varies as $1/(M^A)^{1/2}$ as of course it should. The damping (i.e., the width of the Einstein oscillator peak) depends on M^A roughly as $1/M^A$ (which arises from the $1/M^A$ factor in χ_{22}^{-1}, converting M_{22} to $\tilde{M}_{22}$); this increase of the damping for low diffusing masses fills up the minimum between the diffusion and the oscillator peaks. Finally the area under the curves varies as $1/M^A$, as predicted by (79).

In Fig. 8 we present σ (ω) for various masses of the host ions M^B, while keeping $M^A = 20$, $T = 100$ K, and the elastic constant fixed. This shows an increase in the damping with increasing
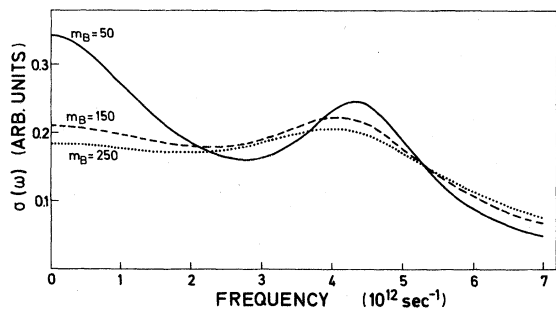
FIG. 8. Conductivity as function of frequency for three different masses for the particles of the host lattice with $A = 2000$ K, $B = 5/a^2$, $a = 3$Å, $M^A = 20$ amu, $M^B c^2 = 6060$ K, $T = 100$ K.

M^B, which arises from the increasing density of phonon states already noted in Sec. IV B.

Similarly in Fig. 9 we show the variation of σ (ω) with the elastic constant of the host, while keeping all the other parameters fixed. This clearly shows the increase of the damping with decreasing c, again arising from the different densities of states available for the decay. Also we note that the Einstein oscillator frequency shifts to lower values as c decreases, in agreement with the flattening of the effective potential in Fig. 1. The area under the curves in Figs. 8 and 9 is constant, in agreement with Eq. (79).

Finally in Fig. 10 we compare the results of our full calculation with the FP results. The problem with such a comparison is that the damping is not known in the FP approximation and a value has to be chosen for it. We take the matrix element $M_{22}''(\omega_1 = 0, k = 0, k = 0)$ which we calculate at $T = 200$ K, namely $0.58 \times 10^{+12}$ sec^{-1}. This tends to minimize the discrepancies at $T = 200$ K. Differences only arise due to the presence of off-diagonal matrix elements and the k dependence of M_{22} (the ω dependence can be neglected in the range
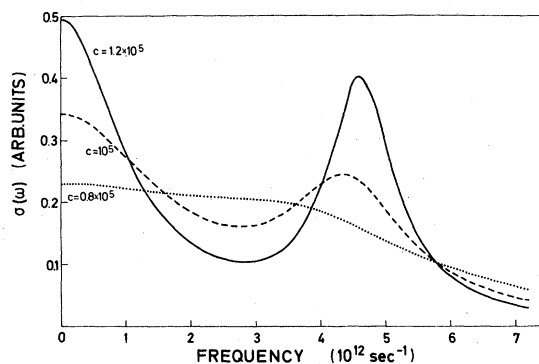
FIG. 9. Conductivity as function of frequency for three different sound velocities (cm/sec) with $A = 2000$ K, $B = 5/a^2$, $a = 3$Å, $M^A = 20$ amu, $M^B = 50$ amu, $T = 100$ K.
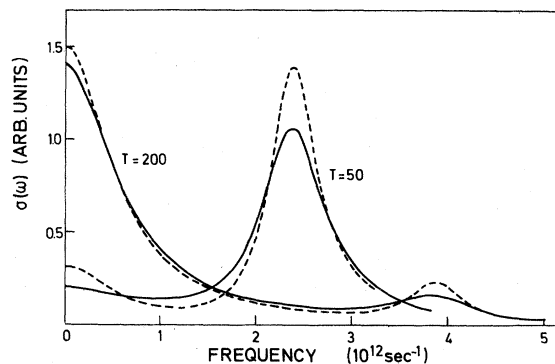
FIG. 10. Conductivity as function of the frequency for two temperatures: — full theory, --- $M_{22}(k_1, k_2, \omega)$ is approximated by its $k_1 = k_2 = \omega = 0$ value. The other parameters are $A = 2000$ K, $B = 5/a^2$, $a = 3$Å, $c = 10^5$ cm/sec, $M^A = M^B = 50$ amu.

of frequencies considered). The full curve shows the calculation with the full M_{22}, and the dashed curve shows the FP approximation. The qualitative agreement is quite good. However, when the temperature is changed to 50 K, the discrepancy at $\omega = 0$ is already 50%. The frequency-dependent conductivity $\sigma(\omega)$ has also been calculated recently by other authors.[15-18] Neglecting phonons, they solved the Fokker-Planck equation for one particle either by a continued fraction method or by expansions in terms of complete sets of functions. Such a treatment has the advantage of yielding accurate numerical values for all temperatures and wave vectors once the approximations behind the Fokker-Planck equation have been accepted. In particular, the damping γ is assumed to be independent of frequency, wave vector, and temperature. In contrast to that, our treatment gives a microscopic foundation of γ in terms of the memory function M^{22}. Moreover, it allows us to calculate M^{22} in a well-defined approximation and thus to determine its dependence on all parameters of interest. Owing to the more complex nature of our approach, we have neglected higher powers in the momenta which means that our results are reliable only for temperatures small compared with E_A. Comparing our results with those of Refs. 15–18 we would like to stress two points: (a) Each of our $\sigma(\omega)$ curves characterized by a certain set of parameters $T, M^A, M^B, c, \ldots$ could be qualitatively reproduced by a curve calculated from the Fokker-Planck equation if an effective γ is used. (b) Our many-body treatment of the memory function M^{22} is, however, necessary if questions like deviations from an Arrhenius law of $\sigma(0)$ or isotopic effects are discussed. This is so because M^{22} itself shows a non-negligible dependence on T and M^A.
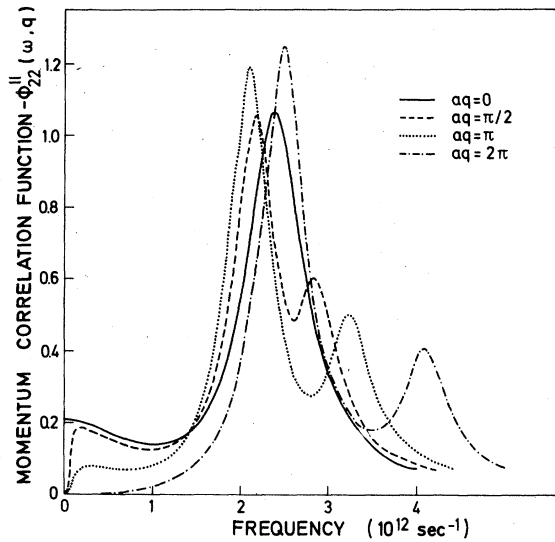
FIG. 11. Momentum correlation function as function of frequency for different momentum transfers with $A = 2000$ K, $B = 5/a^2$, $a = 3$ Å, $c = 10^5$ cm/sec, $M^A = M^B = 50$ amu, $T = 50$ K.

D. Momentum-momentum correlation function $-\Phi_{22}''(q, \omega)$

In this section we discuss the q dependence of Φ_{22}. Figure 11 shows the calculated results for $T = 50$ K. The figure shows that $-\Phi_{22}''(\vec{q}, \omega = 0) = 0$ whenever $\vec{q} \neq 0$, whereas it is finite for $q = 0$. This behavior arises from the importance of the order in which the $\omega \to 0$ and $\vec{q} \to 0$ limits are taken. The various peaks appearing in Fig. 11 can best be understood by referring to the dispersion curves in Fig. 2 which were calculated for the same parameters. Similar to Fig. 6, the main intensity at 50 K is in the peak originating from the Einstein oscillator (the second from the bottom in Fig. 2). There is a gradual transfer of intensity from the diffusive peak to the oscillator peak as q increases so that at $q = \pi/a$ the oscillator peak is more intense. This transfer of intensity is completed at $q = 2\pi/a$, where no intensity is left in the diffusive peak. There is also some contribution from higher dispersion branches, just as in Fig. 6. If even larger values of q were considered, the intensity would begin to shift to the higher dispersion branches. The q dependence of the peak can also be understood immediately by referring to the dispersion curves: As q increases from 0 to π/a, the diffusive peak shifts to higher frequencies and the oscillatory one to lower frequencies.

E. Density-density correlation function

The density-density relaxation function $\Phi_{11}''(q, \omega)$ has much more practical importance than $\Phi_{22}''(q, \omega)$, since it is related directly to the in-
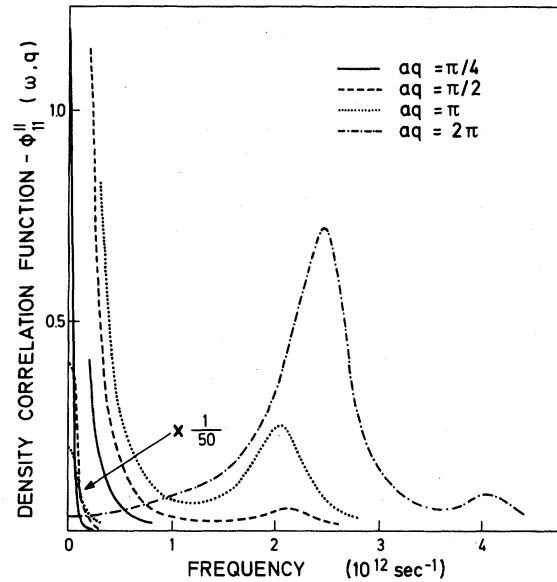
FIG. 12. Density correlation function as function of frequency for different momentum transfers with $A = 2000$ K, $B = 5/a^2$, $a = 3$ Å, $c = 10^5$ cm/sec, $M^A = M^B = 50$ amu, $T = 50$ K.

coherent neutron scattering cross section (64). In Fig. 12 we show the results for $-\Phi_{11}''$ for $T = 50$ K. At $q = 0$ (not shown), Φ_{11}'' is a δ function in the origin, as may be seen by inspection of (79). Ω_{12} contains a factor q and hence vanishes and Φ_{11} reduces to

$$\Phi_{11}(z, 0, 0) = -\chi_{11}/2. \tag{80}$$

For finite q the δ function cancels (except if q is a multiple of $2\pi/a$) and $\Phi_{11}''(\omega = 0, q, q)$ is finite. For small q values Φ_{11}'' consists of a Lorentzian at the origin whose width broadens with increasing q (and increasing temperature). This is the over-damped diffusive peak. At the same time the Einstein oscillator peak gains in intensity $\sim q^2$.

Φ_{11} can be completely understood in terms of the overdamped diffusive peak whose width increases up to $q = \pi/a$ and then decreases again to a δ function at $q = 2\pi/a$, and the Einstein oscillator peak, whose weight increases with q. If q increases, even higher dispersion branches can contribute.

For completeness we would like to compare our results for Φ_{11} with the results for a Chudley-Elliott[20] model, applied to our situation. In the Chudley-Elliott model one uses a convolution approximation between the diffusive and the oscillatory part as

$$\Phi_{11}(\vec{q}, \omega) \sim \int d\omega' \Phi_{11}^D(\vec{q}, \omega') \Phi_{11}^v(\vec{q}, \omega - \omega'), \tag{81}$$

which corresponds to saying that the particle can simultaneously oscillate and diffuse and moves from r_1 to r_2 by diffusing to r' and then oscillating from r' to r_2. The diffusive part is given by diffusive part is given by

$$\Phi_{11}^D(q, \omega) = f(q)/[\omega^2 + f^2(q)], \qquad (82)$$

where

$$f(q) = [1 - \cos(qa)]/\tau \qquad (83)$$

and τ is the jump time. The total relaxation function is then given by

$$\Phi_{11}(q, \omega) \sim f(q) e^{-x} \left(\frac{2}{\omega^2 + f(q)^2} I_0(x) \right.$$
$$\left. + \sum_{\substack{n=1 \\ \pm}}^{\infty} \frac{I_n(x)}{(\omega \pm n\omega_E)^2 + f^2(q)} \right),$$
$$(84)$$

where $x = (k_B T/M^A)(q^2/\omega_E^2)$, ω_E is the Einstein oscillator frequency for a diffusing particle, and I_n are modified Bessel functions. In (84) the term in I_0 corresponds to the zero-phonon term and I_n to the n-phonon terms.

Equation (84) shows that the width of all lines varies as $f(q) \sim q^2$ for small q, not just for the diffusive line. Similar to our results, the intensity of the one-phonon line varies $\sim q^2$ for small q. But the intensity in the phonon lines is much smaller than we would predict (for $T = 90$ K and $aq = \pi$ it is approximately $\frac{1}{5}$th of our result) and it increases rather than decreases with T. Furthermore, there is no dispersion in the peak positions. Whereas for small q values there is reasonable qualitative agreement between the Chudley-Elliott model and our theory (if one uses a suitably chosen τ to get the same diffusion constant), there is not even qualitative agreement for large q values.

In the Chudley-Elliott model the width of the lines is periodic in $aq = 2\pi$. In particular one gets a series of δ functions whenever aq is a multiple of 2π. The intensity of the higher phonon lines increases with increasing q and tends to a constant independent of n for $q \to \infty$. In our model only the $\omega = 0$ peak is a δ function; if aq is a multiple of 2π, the peaks centered at finite frequencies retain a finite width. For increasing q most of the intensity is localized in one or two peaks of Φ_{11}'' (depending on the exact q value), which shifts to higher frequencies as q increases. In particular, the peak at $\omega = 0$ has a very small intensity for

large q values—the intensity varies roughly as $d(G)$ compared to 1 in the main peak.

V. CONCLUSIONS

We have derived a transport theory of a single diffusing ion constrained to move in one dimension in a three-dimensional deformable lattice. Our calculation was based on the Mori formalism with the variables $n(k_x)$ and $p(k_x)$, and the memory kernel was evaluated in the mode-mode coupling approximation.

The memory kernel was found to decrease to zero for frequencies around the highest lattice frequencies and for wave vectors such that the associated diffusion mode corresponds to a similar frequency. Both results differ from the assumptions made in the Fokker-Planck treatment of the problem.

The absolute magnitude of the diffusion constant is found to be of the same order of magnitude as predicted by classical rate theory. An Arrhenius law is a reasonable description of the temperature dependence. However, the activation energy increases slightly with temperature and approaches the barrier height only at very low temperatures. At higher temperatures the lattice relaxation is imperfect, leading to a higher apparent activation energy. This increase of the activation energy depends on the mass of the diffusing ion and thus gives rise to an isotope effect in the activation energy. On the other hand, the prefactor (attempt frequency) varies less with the mass than $(M^A)^{-1/2}$, especially for large M^A. These results show that an analysis of experiments in terms of the classical rate theory may be dangerous. Furthermore our calculations show that one can get an isotope effect for the activation energy even in a purely classical theory. This means that it might not even be necessary to resort to quantum theory to explain the experiments with H, D, and T. We also studied the influence of the mass of the lattice ions and the elastic constant.

The frequency-dependent conductivity shows a two-peak structure. This result is in qualitative agreement with previous Fokker-Planck calculations; however, the two peaks exist for a wider range of parameters in our calculations. For the incoherent neutron scattering we predict a peak centered at $\omega = 0$ whose width increases with wave vector and an Einstein oscillator peak whose weight increases as k^2.

APPENDIX

In the following we derive the explicit from (55) for the memory kernel. If one introduces the abbreviations

$$\Phi_{ik}(t) = \langle A_i | e^{-i\mathcal{L}t} A_k \rangle \tag{A1}$$

and

$$N_{ij,kl} = \langle A_i A_j | A_k A_l \rangle, \tag{A2}$$

one obtains within these approximations

$$M_{22}(z, (k+G_1)_x, (k+G_2)_x) = i\beta^{-1} \int_0^\infty dt\, e^{izt} \langle p((k+G_1)_x)\mathcal{L}Q | A_i A_j \rangle$$
$$\times N^{-1}_{ij,kl}[\Phi_{km}(t)\Phi_{ln}(t) + \Phi_{kn}(t)\Phi_{lm}(t)]N^{-1}_{mn,rs}\langle A_r A_s | Q\mathcal{L}p((k+G_2)_x) \rangle. \tag{A3}$$

$|\mathcal{L}p\rangle$ is symmetric with respect to time reversal, whereas p and P are antisymmetric. Therefore the vertices $\langle A_i A_j | Q\mathcal{L}p \rangle$ vanish, unless none or both the variables A_i and A_j are momenta. On the other hand, we restricted our original set of variables so that it contains only first powers of momenta. Therefore, to be consistent with this original approximation, we keep only products of n and Q. Then we get the following possible combinations:

$$\sum_{q_x, G'_x, G''_x} |n((k+q+G')_x)n((-q+G'')_x)\rangle, \tag{A4a}$$

$$\sum_{\vec{q}, \alpha, \beta} \left| \tilde{Q}\begin{pmatrix} \vec{k}+\vec{q} \\ \alpha \end{pmatrix} \tilde{Q}\begin{pmatrix} -\vec{q} \\ \beta \end{pmatrix} \right\rangle, \tag{A4b}$$

$$\sum_{\vec{q}, G'_x, \alpha} \left| n((k+q+G')_x)\tilde{Q}\begin{pmatrix} -\vec{q} \\ \alpha \end{pmatrix} \right\rangle. \tag{A4c}$$

It is tedious but straightforward to show that $\langle p\mathcal{L}Q | nn \rangle = 0$ and therefore (A4a) does not contribute. (A4b) leads to the vertex

$$\langle p\mathcal{L}Q | \tilde{Q}\tilde{Q} \rangle = -\langle p\mathcal{L}n \rangle \chi^{-1}_{11}\langle n | \tilde{Q}\tilde{Q} \rangle = O(1/N) \tag{A5}$$

if $\langle n | \tilde{Q}\tilde{Q} \rangle$ is factorized. Therefore (A4b) is also neglected. This leaves us with (A4c). The appropriate normalization constant is

$$N\begin{pmatrix} (k+q)_x & -\vec{q} \\ G_x & \alpha \end{pmatrix} \begin{pmatrix} (k+q')_x & -\vec{q}' \\ G'_x & \alpha' \end{pmatrix} = \left\langle n((q-q'+G-G')_x)\tilde{Q}\begin{pmatrix} -\vec{q} \\ \alpha \end{pmatrix} \middle| \tilde{Q}\begin{pmatrix} -\vec{q}' \\ \alpha \end{pmatrix} \right\rangle$$

$$\simeq \delta(q_x - q'_x)\delta_{\alpha\alpha}d(G_x - G'_x)\left\langle \tilde{Q}\begin{pmatrix} -\vec{q} \\ \alpha \end{pmatrix} \middle| \tilde{Q}\begin{pmatrix} -\vec{q}' \\ \alpha' \end{pmatrix} \right\rangle, \tag{A6}$$

where in the last step the factorization approximation was used. We can now define a vertex T by

$$T\begin{pmatrix} (k+G_1)_x & \begin{matrix} (k+q)_x & -\vec{q} \\ G_{2x} & \alpha \end{matrix} \end{pmatrix} = \sum_{G'}\left\langle p((k+G_1)_x)\mathcal{L}Q \middle| n((k+q+G')_x)\tilde{Q}\begin{pmatrix} -\vec{q} \\ \alpha \end{pmatrix} \right\rangle N^{-1}\begin{pmatrix} (k+q)_x & -\vec{q} \\ G'_x & \alpha \end{matrix} \begin{matrix} (k+q)_x & -\vec{q} \\ G_{2x} & \alpha \end{pmatrix} \tag{A7}$$

and propagators by

$$\Phi_{11}(t, (k+G_1)_x, (k+G_2)_x) = \langle n((k+G_1)_x) | e^{-i\mathcal{L}t} n((k+G_2)_x) \rangle, \tag{A8}$$

$$\Phi_{33}(t, \vec{k}\alpha, \vec{k}\alpha) = \left\langle Q\begin{pmatrix} \vec{k} \\ \alpha \end{pmatrix} \middle| e^{-i\mathcal{L}t} \tilde{Q}\begin{pmatrix} \vec{k} \\ \alpha \end{pmatrix} \right\rangle. \tag{A9}$$

If we neglect propagators of the form $\langle n | e^{-i\mathcal{L}t}\tilde{Q} \rangle$, (A3) becomes

$$M_{22}(z, (k+G_1)_x, (k+G_2)_x) = ik_B T \sum_{\vec{q}, G'_x, G''_x, \alpha} T\begin{pmatrix} (k+G_1)_x & \begin{matrix} (k+q)_x & -\vec{q} \\ G'_x & \alpha \end{matrix} \end{pmatrix} T^*\begin{pmatrix} (k+G_2)_x & \begin{matrix} (k+q)_x & -\vec{q} \\ G''_x & \alpha \end{matrix} \end{pmatrix}$$
$$\times \int_0^\infty dt\, e^{izt}\Phi_{11}(t, (k+q+G')_x, (k+q+G'')_x)\Phi_{33}(t, -\vec{q}\alpha, -\vec{q}\alpha). \tag{A10}$$

Let us first evaluate the propagators. By substituting into the equation of motion and assuming that the phonons are not disturbed by the presence of the diffusing particle we get

$$\Phi_{33}(t, \vec{k}\alpha, \vec{k}'\alpha') = \frac{\delta(\vec{k} - \vec{k}')\delta_{\alpha\alpha'}}{M^B \omega^2\left(\begin{smallmatrix}\vec{k}\\\alpha\end{smallmatrix}\right)} \cos\left[\omega\left(\begin{smallmatrix}\vec{k}\\\alpha\end{smallmatrix}\right)t\right]. \tag{A11}$$

If we substitute this we get

$$\int_0^\infty dt\, e^{izt}\Phi_{11}(t, (k+q+G')_x, (k+q+G'')_x)\Phi_{33}(t, -\vec{q}\alpha, -\vec{q}\alpha)$$

$$= \left[i \Big/ 2M^B\omega^2\left(\begin{smallmatrix}\vec{q}\\\alpha\end{smallmatrix}\right)\right]\int d\omega\,(z-\omega)\Big/\left[(z-\omega)^2 - \omega^2\left(\begin{smallmatrix}\vec{q}\\\alpha\end{smallmatrix}\right)\right]\Phi_{11}''(\omega, (k+q+G')_x, (k+q+G'')_x), \tag{A12}$$

where $\Phi_{11}''(\omega, k_{1x}, k_{2x})$ is the imaginary part of the Fourier transform of $\Phi_{11}(t, k_{1x}, k_{2x})$.

For the next step we have to find the vertex. Let us first consider $\langle p\mathcal{L}Q | n\vec{Q}\rangle$:

$$\left\langle p((k+G_1)_x)\mathcal{L}Q \left| n((k+q+G')_x)\vec{Q}\left(\begin{smallmatrix}-\vec{q}\\\alpha\end{smallmatrix}\right)\right\rangle \right. = \left\langle p((k+G_1)_x)\mathcal{L} \left| n((k+q+G')_x)\vec{Q}\left(\begin{smallmatrix}-\vec{q}\\\alpha\end{smallmatrix}\right)\right\rangle\right.$$

$$- \sum_{G_x'', G_x'''}\left\langle p((k+G_1)_x)\mathcal{L}\left| n((k+G'')_x)\right\rangle\right.$$

$$\times \left[\chi_{11}^{-1}((k+G'')_x, (k+G''')_x)\left\langle n((k+G''')_x)\left| n((k+q+G')_x)\vec{Q}\left(\begin{smallmatrix}-\vec{q}\\\alpha\end{smallmatrix}\right)\right\rangle\right.\right.$$

$$\left. + \chi_{13}^{-1}\left((k+G'')_x, \left(\begin{smallmatrix}k_x\\\alpha\end{smallmatrix}\right)\right)\left\langle \vec{Q}\left(\begin{smallmatrix}k_x\\\alpha\end{smallmatrix}\right)\left| n((k+q+G')_x)\vec{Q}\left(\begin{smallmatrix}-\vec{q}\\\alpha\end{smallmatrix}\right)\right\rangle\right].\right.$$

$$\tag{A13}$$

In (A13) we replaced Q by $1-P$. The term multiplying χ_{13}^{-1}, however, vanishes except for $\vec{k}+\vec{q} = 0$ or $\vec{k} = 0$, if it is factorized. Hence, we are going to neglect it. Also, since χ_{13} is of $O(1/\sqrt{N})$, one gets $(\chi^{-1})_{11} = \chi_{11}^{-1} + O(1/N)$ in the second term of (67). Then to $O(1/N)$, Eq. (A13) becomes

$$\left\langle p((k+G_1)_x)\mathcal{L}Q | n((k+q+G')_x)\vec{Q}\left(\begin{smallmatrix}-\vec{q}\\\alpha\end{smallmatrix}\right)\right\rangle = \beta^{-1}\left[(k+q+G')_x\,\chi_{13}\left((-q-G'+G_1)_x\left|\left(\begin{smallmatrix}-\vec{q}\\\alpha\end{smallmatrix}\right)\right.\right)\right.$$

$$- \sum_{G_x'', G_x'''}(k+G'')_x\, d(G_{1x} - G_x'')d^{-1}(G_x'' - G_x''')$$

$$\left. \times \chi_{13}\left((-q-G'+G''')_x\left|\left(\begin{smallmatrix}-\vec{q}\\\alpha\end{smallmatrix}\right)\right.\right)\right]. \tag{A14}$$

By substituting (A14) and (48) into (A7) we obtain the simple expression

$$T\left((k+G_1)_x\left|\begin{smallmatrix}(k+q)_x & -\vec{q}\\ G_{2x} & \alpha\end{smallmatrix}\right.\right) = -iN^{-1/2}Aa^{-3}(\pi/B)^{3/2}(\vec{q} - G_{1x}\vec{e} + G_{2x}\vec{e})_x\,(\vec{q} - G_{1x}\vec{e} + G_{2x}\vec{e})_\alpha \exp[-(\vec{q} - G_{1x}\vec{e} + G_{2x}\vec{e})^2/4B].$$

$$\tag{A15}$$

Finally, substituting (A12) and (A15) into (A10), replacing the sum over intermediate $\vec{q}$ by an integral, and performing the integral over the normal directions of $\vec{q}$ (q_y, q_z), we get for the imaginary part of M_{22},

$$M''_{22}(\omega_1, (k+G_1)_x, (k+G_2)_x)$$

$$= -\frac{k_B T A^2 \pi}{16 M^B c^2 a^3 B^3} \sum_{\vec{G}', \vec{G}''} \exp[-(\vec{G}'^2 + G''^2)/4B]$$

$$\times \int_{-q_m}^{q_m} dq_x (q - G')_x (q - G'')_x \exp[q_x(G' + G'')/2B]$$

$$\times \int_{cq_x}^{\omega_D} d\omega\, \omega^{-1} e^{-\omega^2/2Bc^2} \left\{ \left[\left(\frac{\omega}{c}\right)^2 + \vec{G}' \cdot \vec{G}'' - q_x(G' + G'')_x \right] I_0(x) - 2Bx I_1(x) \right\}$$

$$\times [\Phi''_{11}(\omega + \omega_1, (k+q+G'+G_1)_x, (k+q+G''+G_2)_x) + \Phi''_{11}(\omega \rightarrow -\omega)], \qquad (A16)$$

where $x = [(\omega/c)^2 - q_x^2]^{1/2}(\vec{G}' + \vec{G}'')_\perp/2B$. G'_x is the x component and $G'_\perp$ is the normal component of the reciprocal-lattice vector $\vec{G}'$. q_m is the maximum vector of the Debye spectrum and ω_D is the Debye frequency.

[1] *Diffusion in Solids: Recent Developments*, edited by A. S. Nowick and J. J. Burton (Academic, New York, 1975).

[2] *Hydrogen in Metals, Basic Properties*, Topics in Applied Physics, edited by J. Völkl and G. Alefeld (Springer, Berlin, 1978), Vol. 28.

[3] *Superionic Conductors*, edited by G. D. Mahan and W. L. Roth (Plenum, New York, 1976).

[4] J. B. Boyce and B. A. Huberman, Phys. Rep. **51**, 190 (1979).

[5] H. A. Kramers, Physica (Utrecht) **7**, 284 (1940).

[6] G. H. Vineyard, J. Phys. Chem. Solids **3**, 121 (1957).

[7] S. Rice, Phys. Rev. **112**, 804 (1958).

[8] I. Prigogine and T. A. Bak, J. Chem. Phys. **31**, 1368 (1959).

[9] D. M. Rockmore and R. E. Turner, Physica (Utrecht) **29**, 873 (1963).

[10] H. Mori, Prog. Theor. Phys. **33**, 423 (1965).

[11] H. Mori, Prog. Theor. Phys. **34**, 399 (1965).

[12] D. Forster, *Hydrodynamic Fluctuations, Broken Symmetry, and Correlation Functions* (Benjamin, London, 1975).

[13] W. Goetze and K. H. Michel, in *Dynamical Properties of Solids*, edited by G. K. Horton and A. A. Maradudin (North-Holland, Amsterdam, 1974), Vol. 1, p. 499.

[14] W. Goetz and M. Lücke, Phys. Rev. A **11**, 2173 (1975).

[15] P. Fulde, L. Pietronero, W. R. Schneider, and S. Strässler, Phys. Rev. Lett. **35**, 1776 (1975).

[16] W. Dieterich, I. Peschel, and W. R. Schneider, Z. Phys. B **27**, 177 (1977).

[17] W. Dieterich, T. Geisel, and I. Peschel, Z. Phys. B **29**, 5 (1978).

[18] H. Risken and H. D. Vollmer, Z. Phys. B **31**, 209 (1978).

[19] W. G. Kleppmann and H. Bilz, Commun Phys. **1**, 105 (1976).

[20] C. T. Chudley and R. J. Elliott, Proc. Phys. Soc. London **77**, 353 (1961).